Operator-based robust nonlinear control of uncertain wireless power transfer systems

February, 2019

Xudong Gao

The Graduate School of Engineering
(Doctor's Course)

TOKYO UNIVERSITY OF
AGRICULTURE AND TECHNOLOGY

Acknowledgements

For me, studying in Tokyo university of agriculture and technology has been a privilege as well as a remarkable experience.

First, I want to take this opportunity to express my sincere thanks to my supervisor, Professor Mingcong Deng, because of his professionalism and dedication extended to me during my study. Without his constant encouragement and guidance, my academic pursuit would have been much more difficult. Professor Mingcong Deng is a man of vision and principle, I have learned so much from him over the years, like industriousness and attentiveness. He has walked me through all the hardships and setbacks occurred in the study course with his profound knowledge. He always inspires me to go far, and this inspiration has been and will always be a treasure for me.

Second, I want to show my real gratitude to a brilliant array of professors in the university. All of them have deepened my admiration for science, I want especially, to thank Professor Shinji Wakui, Ken Nagasaka, Yosuke Tanaka, Takuji Arima for their brilliant comments on my dissertation, which have greatly enabled me to improve the dissertation for better.

Next, I am indebted to Dr. Fazhan Tao, Dr. Yanfeng Wu, Dr. Mengyang Li, Mr. Guang Jin, Mr. Guanqiang Dong, Mrs. Ximei Li for their able cooperation and assistance. We have worked together, suffered the frustration of our work together and shared the joy of our every little success together. Their company has colored my campus life, making the academic path more vibrant and delightful.

Last but not least, as is true of each stage of education I have completed, I am grateful to my family back in China, more than I can express clearly. They have always remained solid backup for my all activities in this foreign land, both spiritually and materially. Though little does they know about my studies and research, they have shown unwavering support from the very beginning. They have made what I am today. Without them, nothing is impossible in the first place, for which and their unconditional love and encouragement, they have my lifetime gratitude.

Summary

This dissertation provides the operator-based robust nonlinear control design schemes for uncertain wireless power transfer (WPT) systems which is driven by the duty cycle of the switch. The aim of this dissertation is to guarantee the robust stability of the uncertain WPT control systems. Besides, the desired output tracking performance and the high efficiency of the WPT system can be obtained.

Nowadays, there are many challenges such as weight, cost, and inconvenience existing for batteries. WPT systems could be used to continuously charge a electronic device and power the batteries without wires between the transmit side and the receive side, so the researches on designing reliable and effective control to achieve desired output tracking and high efficiency of WPT systems have drawn much attention in recent years. However, the challenging issue still exists, because that the control design system should get the desired performance with consideration of the uncertainties and nonlinearities. To deal with the uncertainties and nonlinearities, operator theory was adopted to the WPT system with uncertainties because of its effectiveness in robust stability of nonlinear systems.

First, the mathematical modeling for WPT systems using the DC-DC circuit is derived. After that, based on operator theory, a proposed robust nonlinear control method is given to tackle the uncertain mutual inductance using sliding mode control method, the uncertain term is resulted from the inaccurate distance between the resonant coils in the nonlinear WPT system. There are two advantages. First, to deal with the uncertain mutual inductance, operator-based right coprime factorization approach is adopted to guarantee the robust stability of the feedback nonlinear system. Besides, sliding mode control (SMC) method was used to obtain the tracking performance in the control system. Moreover, simulations and experiments of the

WPT system are conducted using the proposed control design scheme. The results confirm the effectiveness of the proposed control design scheme.

Second, due to the inherent shortage of traditional SMC technology, the chattering phenomenon existed by using the above operator-based control design scheme. To tackle with the chattering problem, a new operator-based nonlinear robust control design scheme for WPT systems with uncertainties is proposed, where, from different viewpoint, the considered nonlinear system is of Input-Output presentation. The robust stability can be guaranteed by using operator-based robust right coprime factorization approach. Moreover, the tracking performance is improved by using the proposed control design scheme. Simulations and experiments are tested to confirm the effectiveness of this proposed method.

Third, an operator-based optimal equivalent load tracking control scheme is proposed for WPT systems with uncertainties. In the control design systems, the robust stability of the feedback nonlinear control system is guaranteed by using robust right coprime factorization approach. Especially, the impedance matching of the WPT system can be obtained without the acquisition of the AC signal, thus high efficiency can be obtained and the complexity of the setup can be alleviated. Moreover, the desired output voltage can be obtained in the WPT system. Simulations are tested to confirm the effectiveness of this proposed method.

In summary, the dissertation proposes three kinds of operator-based robust nonlinear control design schemes for WPT systems. The first control scheme is focus on ensuring the robust stability of the uncertain WPT systems, the second control method is to improve the tracking performance of the uncertain WPT systems on chattering problem, and the third control scheme aims to obtain desired output voltage and optimal equivalent load, thus desired power and high efficiency using operator-based robust nonlinear control design scheme at the same time. The formal two kinds of control design schemes are validated by both simulations and experiments, the third control system is confirmed by simulations, the results are shown to confirm that the proposed control design schemes are effectiveness.

Contents

List of Figures

Chapter 1

Introduction

1.1 Background

Nowadays, as one of the most promising power sources, batteries are facing some challenges, such as weight, cost, limited energy, reliability [1]. Wireless power transfer system (WPT) could not only be used to charge without wires, but also provide a new way in management of power [2]. There are three main types of WPT techniques according to the transfer distance: far-field, near-field, and mid-range.

Electromagnetic radiation could used deliver power to large volumes of space in far-field WPT system [3–5]. However, the tradeoff between transfer efficiency and directionality should be dealt with. For example, radio-frequency broadcast approach could transfer power anywhere in a specified area when the omnidirectional pattern is selected in transmit side. The mobility is obtained in this situation [6]. However, the efficiency would be low due to the decreasing of the power density. On the other hand, antennas could be used to transfer power as long as several kilometers with efficiency which is more than 90% only when the line-of-sight connection should be accurately determined [7], but the need for alignment equipment and sophisticated tracking in complex environments is suffered.

Inductive power transfer could be used to transfer power in near-field PWT system [8–11]. The architecture is generally used with two coils, and the basic structures have series (S)- S, S -parallel (P), P-S, P-P. To enhance power transfer, the coil in receive side should be selected at the operating frequency. Besides, the parasitic capacitor of transmitter need to be selected to compensate the transmit inductor and the reflected inductor, thus the imaginary power in some structures could be eliminated. Moreover, the frequency used in the WPT system is generally in KHz range, and ferromagnetic materials are always adopted to improve the coupling, then the power transfer could be enhanced [12]. The quality factors in the mode are usually used under 10, so the transfer efficiency decrease precipitously when the transfer distance is increased. The effective transfer distance is normally within 20 cm [13, 14].

As a novel mode, strongly coupled magnetic resonance (SCMR) technology serves a power transfer way in mid-range WPT applications [15–18]. There are many meaningful results about SCMR, they includes the analyses principle, transfer characteristics, interference and practical applications. The SCMR are always analysed by using either coupled mode theory or circuit theory [19–22], circuit theory is more suitable on analysing the transient state sometimes than coupled mode theory, so circuit theory is popular. Compared with inductive power transfer method, diverse system structures are used in SCMR to realize impedance matching so that high efficiency could be obtained [23–26]. The operating frequency is always in MHz range due to the existence of parasitic capacitors, as a result, the quality factor is high compared with the inductive power transfer. When distance between the coils are increased, the sharp decrease of the transfer efficiency could be alleviated due to the high quality factors. Thus the high efficiency can be obtained in meter range. Because SCMR mode has the advantages, such as the mid-range power transfer, convienience and high efficiency. It is widely used in various areas including charging to the implanted micro-system in the organism in medical implantation applications, to robots and personal digital equipment in industrial and consumer applications, and to conveniently transfer power without wire so that the dangerous could be avoided in transportation applications [27–30]. Impedance matching and stability are two main indexes in WPT systems, impedance matching could be used to obtain the high efficiency of the WPT system [31–34, 49], and the stability of the output voltage should be considered at the same time. In order to obtain impedance matching and guarantee the stability of the uncertain WPT system, one closed-loop control design system is necessary to be designed so that good performance could be achieved, it is an open and challenging problem in WPT systems.

1.2 Current development of wireless power transfer control

For the close-loop control design schemes of WPT systems, there are two main approach to regular the output power and the efficiency of the nonlinear WPT systems. One way is to frequency splitting method, and the other one is impedance matching method. In frequency splitting control system [35–37], the working areas are classified into three areas: over-coupled area, critically-coupled point, and under-coupled areas. By using this method, the high power transfer could be realized twice in over-coupled area by tuning the operating frequency, and critically-coupled point could help realize the high power transfer only once. However, in under-coupled area, both the transfer power and the transfer efficiency would decrease no matter how larger or small the operation frequency is, because the mutual inductance is small. So it is only available in an over-coupled area. As WPT system is difficult to be limited in over-coupled area, it could not be suitable for all the WPT system.

As the other main approach, impedance matching method is very popular in WPT control systems [38–42]. Impedance matching is the approach of designing the input impedance of a special electronic component to realize the maximization of power transfer and minimization of signal reflection. Impedance matching could be realized by various methods: resonance frequency of resonance components tuning method, adjusted of relative distance or angles between adjacent coils, anti-parallel resonant structure method, DC-DC method, and so on. By tuning the resonance frequency of resonance components, the impedance matching can be obtained, thus the high efficiency of the WPT system can be achieved. But the experiments has many resonance components with different values to connect or cut off at each time, but the implement of such experiments is difficult and the accuracy could not be guaranteed. An adjusted of relative distance and angles between transmit and receive coil was proposed. But it is difficult to realized in applications, because the complicated control system and the accurate actuators are necessary. An anti-parallel resonance structure with forward and reverse drive coils, which could alleviate the mutual inductance when the distance between coils is changed. However, the transfer efficiency and power is not considered. And the DC-DC converter could be adopted to realize impedance matching with the adjustable duty cycle. In the above methods mentioned, it is the most promising method by adopting a DC-DC circuit, because not only realize impedance matching can be realized, but also the power management can be obtained [43, 44]. Moreover, DC-DC method is advantageous due to the large distance separation, simple setup and the capibility to control the parameters using a continuous method [45, 46]. So a closed-loop control design scheme is adopted to realize the management of transfer power and efficiency by using DC-DC circuits in this dissertation.

There are different closed-loop feedback control design schemes in WPT systems with DC-DC converters, such as proportional-integral-derivative (PID) control scheme, hysteresis method, perturbation and observation control scheme, and sliding mode control (SMC) scheme [47–49]. The PID control scheme was proposed in a WPT system to realize power management. However, it costs a long time to obtain the desired performance because of the inherent shortage about the PID controller. Hysteresis method is used in a WPT system with a boost circuit to realize the desired transfer power, but the stability of the WPT system was not considered with the switch's infinite frequency in practice. Proportional-and-observations method is widely used in WPT system with buck circuit, boost circuit, and buck-boost circuit, the maximum efficiency and desired power could be obtain at the same time. However, the time to search is long and the settling transien period is needed. Also, SMC scheme is a promising way adopted in WPT system with DC-DC circuits because of the fast dynamic response and simple implementation. But the accurate distance between coils are difficult to achieved in the WPT experiments. Besides, the mutual inductance is very sensitive to the inaccurate distance. What's worse, the output load is inconstant during charging. So there exist uncertain terms in the WPT system. So the robust stability can not be obtained. Moreover, not only the output voltage could be regulated to the desired value, but also the impedance matching should be achieve at the same time. So one more control in transmit side was adopted in the WPT system to obtain both the desired output voltage and impedance matching. However, the high AC (alternating current) frequency signal should be dealt with, thus the complexity of the control system would increase. So it is difficult to design a stable and robust controller for the nonlinear uncertain WPT system using traditional methods.

For nonlinear systems, operator theory is an effective method to guarantee their bounded input bounded output stable using robust right coprime factorization approach [50–53]. Then the tracking of output considering the disturbance in the nonlienar system was developed, so the operator-based nonlinear control approach becomes more effective and comprehensive with such extensions. Because it is usefulness in robust stability, the operator-based right coprime factorization could be adopted in many practical applications, such as a multitank process, a miniature pneumatic curling rubber actuator and a L-shaped arm.

1.3 Motivation

The WPT systems with DC-DC circuit, which driven by the duty cycle of switch, are conducted in this dissertation. Noted that the WPT system is a digital system which is implemented under the sampling and control pattern [54,55]. In the WPT systems, the uncertain terms about the distance between coils (mutual inductance) and variation of output load should be dealt with. It is necessary to propose suitable closed-loop control schemes to realize the power management of the WPT system.

First, motivated by operator theory for uncertain nonlinear systems, rare research on WPT system are conducted considering the uncertain term resulting from the uncertain distance between coils. Besides, SMC scheme serves a promising way to realize the tracking performance, it is advantageous due to the fast dynamic response and simple implement in setup [56–60]. The main challenging is to adopt SMC scheme and operator theory in the uncertain nonlinear control systems, so both the tracking performance of output voltage and robust stability could be guaranteed for the uncertain WPT systems.

Then the chattering phenomenon exists because of the inherent shortage of traditional SMC technology in our fist step [70, 71, 77]. Motivated by the elimination method of chattering phenomenon existing in traditional SMC technology, the tracking performance could be improved by eliminating the chattering phenomenon. It is difficult to tackle the uncertain term and improve the tracking performance of output voltage at the same time.

Moreover, only the tracking performance of output voltage is obtained for the robust WPT control system by using the above two proposed control schemes, the impedance matching may be destroyed when the output load is varied. Besides, high frequency AC (alternating current) signal increase the complexity of the setup [61]. Motivated by the power management of both transfer power and efficiency [62, 63], not only the tracking performance of output voltage should be obtained, but also the impedance matching need to be realized when the output load varies, and the acquisition of high frequency AC signal should be eliminated. Furthermore, the uncertain term of the WPT systems need to be dealt with.

To sum up, this dissertation adopted the operator-based robust nonlinear control scheme, sliding mode control, and impedance matching in control design for uncertain WPT systems, and confirm their effectiveness in simulations and/or experiments. The research is aim to realize desired output voltage, maximize the efficiency, and robustness of the uncertain WPT system.

1.4 Contributions

This dissertation proposes the operator-based robust nonlinear control schemes for uncertain WPT systems. There are three main contributions which are shown as follows.

First, to tackle the uncertain mutual inductance, which is caused by the inaccurate distance between the transmitter and receiver in WPT systems, the operator-based robust nonlinear control design scheme is proposed by using sliding mode control method. By using the proposed control design scheme, the robust stability of the WPT system with the uncertain term could be guaranteed. Besides, we could also obtain the desired tracking performance by using sliding mode control method. The simulations and experiments show the effectiveness of the proposed control scheme [64, 65].

Second, to solve the chattering probem in the above proposed control design system, one new robust nonlinear control scheme is proposed to eliminate the chattering problem for WPT systems with uncertaint terms. By using the new robust nonlinear control scheme, the robust stability can be guaranteed by using operator-based robust right coprime factorization approach. Besides, the tracking performance is improved. Simulations and experiments are presented to show the avaliable of this proposed control design system [66].

Third, an optimal equivalent load tracking control scheme based on operator theory is proposed for WPT systems with the uncertain term. By using the robust nonlinear control scheme, the robust stability of the feedback nonlinear control system is obtained by using robust right coprime factorization approach. Besides, the impedance matching could be obtained for the coupling system, and the acquisition of the AC signal can be eliminated, thus high efficiency could be got and complexity of the setup can be eliminated. At the same time, the desired output voltage could be tracked in the WPT system. Simulations are tested to confirm that the the proposed control design scheme is effectiveness [67–69].

1.5 Organization

The organization of the rest dissertation can be summarized as follows:

In Chapter 2, the basic definitions and key theories are provided for mathematical modeling of the WPT system and control design scheme in the dissertation. Circuit theory is employed to model the power management of the WPT system. Then some basic definition and notations for operator theory are presented. Moreover, the method to realize impedance matching for the

WPT system is given by tuning the duty cycle of DC-DC circuit. After that, the problem statement is given.

In Chapter 3, the mathematical modeling of WPT system with buck circuit is derived. According to the modeling, by using sliding mode technology, an operator-based robust nonlinear control scheme is proposed. There are two aims: one aim is to deal with the uncertain term caused by the inaccurate distance between coils, the other one is to obtain the desired tracking performance. Both simulations and experiments are presented to confirm the effectiveness of this proposed control design system.

In Chapter 4, to eliminate the chattering problem existing in traditional SMC method, a new robust control design scheme based on operator theory for uncertain WPT systems is proposed, where, from different viewpoint, the considered nonlinear system is of Input/Output presentation. The robust stability is guaranteed by using operator-based robust right coprime factorization approach. Moreover, the tracking performance can be improved when compared to the previous method on chattering phenomenon. The results of the simulations and experiments are conducted to verify its effectiveness.

In Chapter 5, to realize both desired output voltage and high efficiency of the WPT systems, an operator-based optimal equivalent load tracking control scheme for uncertain wireless power transfer systems is proposed. When the proposed control design scheme is adopted, the uncertain term could be dealt with by using the robust right coprime factorization approach, so the robust stability could be obtained. Then the optimal equivalent load for the coupling system can be matched to realize impedance matching without the acquisition of alternating current signal, thus the high efficiency could be obtained. Moreover, the reference output voltage can be tracked. Simulations are presented to verify that the proposed control design system is effectiveness.

In Chapter 6, the proposed operator-based robust nonlinear control design schemes are summarized. It could be concluded that by using the proposed control design schemes, the uncertain term is dealt with, desired tracking performance of output voltage is obtained. Moreover, the impedance matching could be maintained at the same time, thus high efficiency is obtained. Simulations and/or experiments have confirm their effectiveness.

Chapter 2

Mathematical preliminaries and problem statement

2.1 Introduction

In this chapter, the mathematical preliminaries and theoretical background to remaining the following chapters of this dissertation is presented. It also provides the foundation for other research topics in WPT system control design system.

In Section 2.2, the circuit theory is introduced to analyze the power exchange between two resonance objects to model the coupling system of the WPT systems.

In Section 2.3, the mathematical modeling of buck circuit is presented in its transient state.

In Section 2.4, the basic definitions of operator theory based right factorization, right coprime factorization, and robust right coprime factorization for nonlinear systems are introduced. Then the bounded input bounded output (BIBO) stable of the uncertain nonlinear systems could be achieved by using these theories.

In Section 2.5, the impedance matching theory using buck circuit is given to achieve a high efficiency for WPT system.

In Section 2.6, the problem discussed in this dissertation is presented.

In Section 2.7, the conclusion of this chapter is presented.

2.2 Circuit theory

Series-series compensation is one of the basic structure in WPT systems, The equivalent circuit of the coupling system between two coils is shown in Fig. 2.1. V_s is the AC source, L_1 and L_2 are the inductors of transmit inductor and receive inductor, C_2 and C_3 mean the compensated capacitor for transmit inductor and receive inductor, R_2 and R_3 represent the parasitic resistance of the two coils. Figs. 2.2 and 2.3 are the simplified equivalent models of Fig. 1a by using the bidirectional reflected load approach, where V_{ref}, R_{ref1}, R_{ref2}, $Z_2(Z_3)$ and w are the reflected source voltage from transmit side to the receive side, the reflected load form the receive side to transfer side, the reflected load from transmit side to receive side, the total load in transmit (or receive) side, and the system operating frequency, respectively.

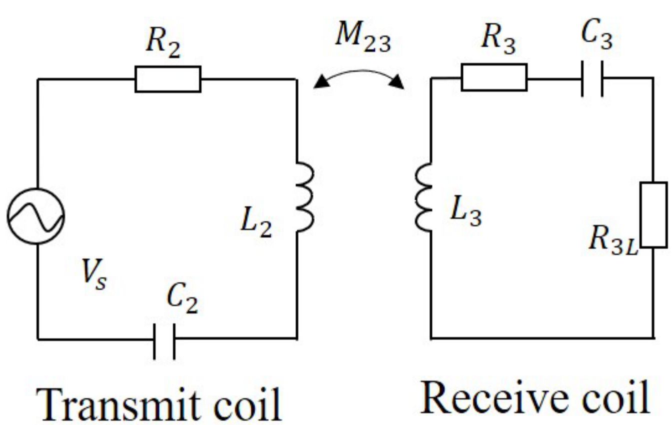

Figure 2.1: Equivalent circuit of the basic 2-coil WPT system

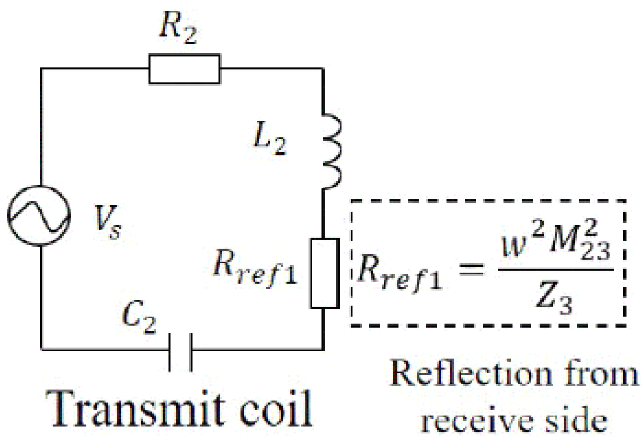

Figure 2.2: Simplified circuit in transmit coil

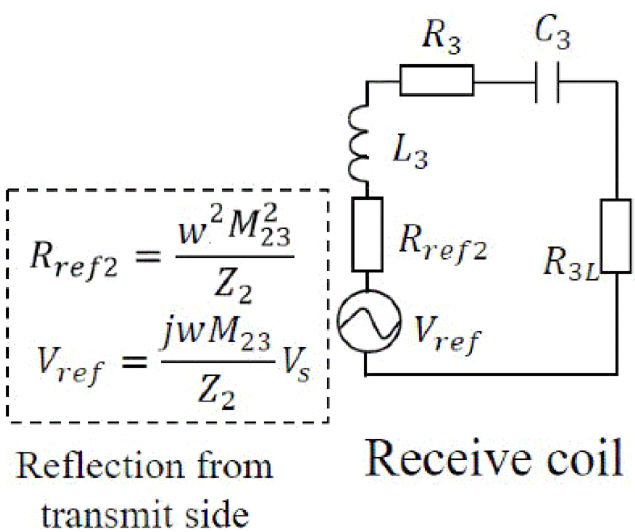

Figure 2.3: Simplified circuit in receive coil

For WPT systems, the LC structure is always tuned using the same operating frequency ($w = 1/\sqrt{L_2C_2} = 1/\sqrt{L_3C_3}$) to obtain the high efficiency. The reflected load from the receive side to the transmit side can be shown as follows.

$$R_{ref1} = \frac{w^2M_{23}^2}{R_3 + R_{3L}} \tag{2.1}$$

$$\eta = \frac{w^2M_{23}^2R_{3L}}{(R_3 + R_{3L})[w^2M_{23}^2 + (R_3 + R_{3L})(R_2 + R_s)]} \tag{2.2}$$

By taking derivative of equation about efficiency with respect to R_{3L}, the optimal value of the load $R_{3L,opt}$ for high transfer efficiency is as follows.

$$R_{3L,opt} = R_3\sqrt{1 + \frac{(wM_{23})^2}{R_2R_3}} \tag{2.3}$$

2.3 Mathematical modeling of buck circuit

Buck circuit adopted in this dissertation as the DC-DC circuit is depicted as in Fig. 2.4.

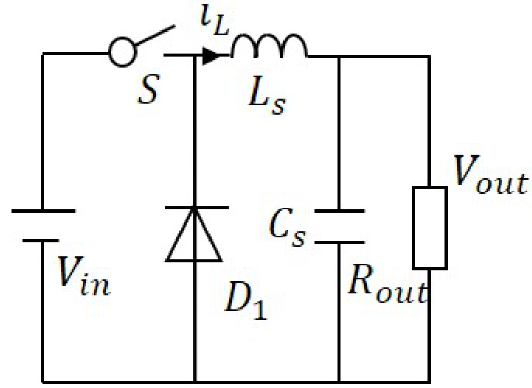

Figure 2.4: Equivalent circuit of buck circuit

Then the mathematical modeling of the circuit is as follows.

$$\begin{aligned} \frac{di_L}{dt} &= \frac{1}{L}(uV_{in} - V_{out}) \\ \frac{dV_{out}}{dt} &= \frac{1}{C}(i_L - \frac{V_{out}}{R_{out}}) \end{aligned} \tag{2.4}$$

As well known in electrical theory, the function of buck circuit is to convert input voltage into lower output voltage by tuning the duty cycle D_3 ($0 < D_3 < 1$) of switch. Besides, the input power equals the output power when the buck circuit is considered as lossless. Then the following equations could be obtained.

$$\begin{aligned} V_{out} &= D_3 V_{in} \\ V_{in} I_{in} &= V_{out} I_{out} \end{aligned} \tag{2.5}$$

So the input impedance of the buck circuit is as follows.

$$Z_L = \frac{R_{out}}{D_3^2} \tag{2.6}$$

It should be noted, Z_L is always larger than R_{out}. So R_{out} value of this WPT system selected must be smaller than designed input impedance Z_L.

2.4 Operator-based robust nonlinear control approach

2.4.1 Definitions on spaces

In this section, some basic linear spaces used in operator theory are introduced as follows.

Normed linear space

Consider a space X of time functions. If X is closed under addition and scalar multiplication, it could be defined as a vector space. The space X is said to be a normed linear space if each element x in X is endowed with norm $\| \cdot \|_X$, which can be defined in any way so long as the following three conditions are satisfied.

1) $\| x \|$ is a real, positive number and is different from zero unless x is identically zero.

2) $\| ax \| = |a| \, \| x \|$.

3) $\| x_1 + x_2 \| \leq \| x_1 \| + \| x_2 \|$.

Banach space

Banach space is defined as a complete normed space. It is a vector space X over the real or complex numbers with a norm $\| \cdot \|$ such that every Cauchy sequence (with respect to the metric $d(x, y) = \|x - y\|$) in X has a limit in X. Many spaces of sequences or functions are infinite dimensional Banach spaces.

Extended linear space

Let Z be the family of real-valued measurable functions defined on $[0, \infty)$, which is a linear space. For each constant $T \in [0, \infty)$, let P_T be the Projection operator mapping from Z to another linear space, Z_T, of measurable functions such that where, $f_T(t) \in Z_T$ is called the truncation of $f(t)$ with respect to T. Then, for any given Banach space X of measurable function, if

$$X_e = \{ f \in Z : \| f_T \|_X < \infty, \quad for\ all T < \infty \} \tag{2.7}$$

The extended linear space is used in this dissertation because the sampling time is finite-time in experiments.

2.4.2 Definitions of operators

Let the spaces U and Y be two extended normed linear spaces of complex numbers, and let U_s and Y_s be normed linear subspaces, called the stable subspaces of U and Y.

Operator:

Define the operator $Q : U \to Y$ be a mapping from input space U to output space Y. The operator Q can be expressed as $y(t) = Q(u)(t)$ where $u(t)$ is the element of U and $y(t)$ is the element of Y. The operators are all assumed to be casual, well-posed and bounded. $D(Q)$ and $R(Q)$ denote the domain and range of operator Q, respectively.

Bounded input bounded output (BIBO) stability:

Let Q be a nonlinear operator with $D(Q) \subseteq U^e$ and $R(Q) \subseteq Y^e$. If $Q(U) \subseteq Y$, Q is said to be stable. If Q maps all input functions from U_s into the output space Y_s, then operator Q is said to be bounded input bounded output stable or simple stable. Otherwise, the Q could not map all input functions from U_s into the output space Y_s, Q is unstable. All the stable operators mentioned in this dissertation mean BIBO stable.

Invertible:

An operator Q is said to be invertible if there exists an operator P such that

$$Q \cdot P = P \cdot Q = I. \tag{2.8}$$

P is called the inverse of Q and is denoted by Q^{-1}, where, I is the identity operator, and $Q \cdot P$ is an operation satisfying

$$D(Q \cdot P) = P^{-1}(R(P) \bigcap D(Q)). \tag{2.9}$$

Unimodular operator:

Let $S(U, Y)$ be the set of stable operators mapping from U to Y. Then, $S(U, Y)$ contains a subset defined by

$$\mu(U, Y) = \left\{ M : M \in S(U, Y),\ M \textit{ is invertible with } M^{-1} \in S(U, Y) \right\}. \tag{2.10}$$

Elements of $\mu(U, Y)$ are unimodular operators.

Lipschitz operator:

For any subset $D \subseteq U$, let $F(D, Y)$ be the family of nonlinear operators Q such that $D(Q) = D$ and $R(Q) \subseteq Y$. The (semi)-norm on (a subset of) $F(U_s, Y_s)$ is denoted by

$$\| A \| := \sup_{\substack{u_1, u_2 \in \mathbf{U} \\ u_1 \neq u_2}} \frac{\| Q(u_1) - Q(u_2) \|_Y}{\| u_1 - u_2 \|_U}, \tag{2.11}$$

if it is finite. In general, it is a semi-norm in the sense that $\|Q\| = 0$ does not necessarily imply $Q = 0$. In fact, it can be easily seen that $\|Q\| = 0$ if Q is a constant operator (need not to be zero) that maps all elements from D to the same element in Y.

Let $Lip(D, Y)$ be the subset of $F(D, Y)$ with all elements Q satisfying $\|Q\|\infty$. Each $Q \in Lip(D, Y)$ is called a Lipschitz operator mapping from D to Y, and the number $\|Q\|$ is called the Lipschitz semi-norm of the operator Q on D.

Generalized Lipschitz operator:

Let X^e and Y^e be extended linear spaces associating respectively with two given Banach spaces X and Y of measurable functions defined on the time domain $[0, \infty)$, and let D be a subset of X^e. A nonlinear operator $Q : D \to Y^e$ is called a generalized Lipschitz operator on D if there exists a constant L such that

$$\| [Q(u_1)]_T - [Q(u_2)]_T \| \leq L \| u_1 - u_2 \| \tag{2.12}$$

for all u_1, u_2 and for all $T \in [0, \infty)$. Noted that the least such constant L is given by the norm of Q with

$$\begin{aligned} \| Q \|_{Lip} &= \| Q(u_0) \|_Y + \| Q \| \\ &= \| Q(u_0) \|_Y \\ &\quad + \sup_{T \in [0,\infty)} \sup_{\substack{u_1, u_2 \in \mathbf{U} \\ u_1 \neq u_2}} \frac{\| Q(u_1) - Q(u_2) \|_Y}{\| u_1 - u_2 \|_U} \end{aligned} \tag{2.13}$$

for any fixed $u_0 \in D$.

Based on (2.13), it follows immediately that for any $T \in [0, \infty)$

$$\begin{aligned} \| [Q(u_1)]_T - [Q(u_2)]_T \| &\leq \|Q\| \ \| u_1 - u_2 \|_X \\ &\leq \|Q\|_{Lip} \ \| u_1 - u_2 \|_X \ . \end{aligned} \tag{2.14}$$

Lemma 2.1 Let X^e and Y^e be extended linear spaces associating respectively with two given Banach spaces X and Y, respectively, and let D be a subset of X^e. The following family of Lipschitz operators is a Banach space:

$$Lip(D, Y^e) = \{Q : D \to Y^e \quad \|Q\|_{Lip} < \infty \ on \ D\}. \tag{2.15}$$

2.4.3 Right coprime factorization

As shown in Fig. 2.5, define a nonlinear system as operator $P : U \to Y$. U and Y are the input and output space of this plant.

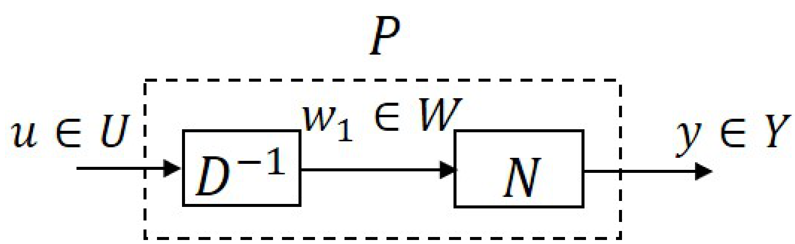

Figure 2.5: Right factorization of the plant

Right factorization:

If there exists a linear space W, operators $D : W \to U$ which is also invertible, and $N + \triangle N : W \to Y$ so that $P + \triangle P = (N + \triangle N)D^{-1}$, the plant is said to have a right factorization [78–82].

Right coprime factorization:

Let (N, D) be the right factorization of P. The feedback nonlinear control system shown in Fig. 2.6 is BIBO stable if there exist two stable operators

$A : Y \to U$ and $B : U \to U$ (B is also invertible) satisfying the following equations [83–86].

$$AN + BD = M \tag{2.16}$$

where M is an unimodular operator.

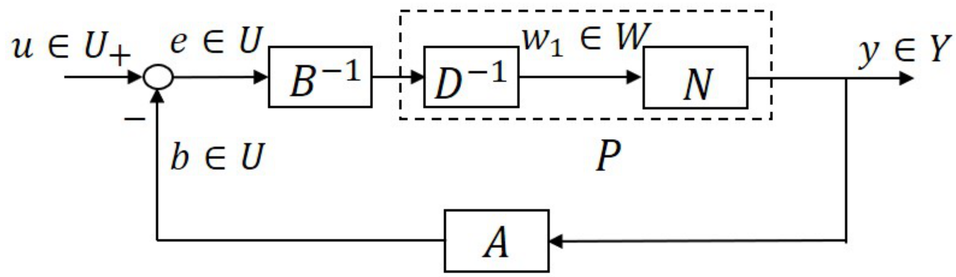

Figure 2.6: Feedback nonlinear system of the plant

Robust right coprime factorization:

To consider the uncertain term in the nonlinear system. With the designed operators A and B in Fig. 2.7, the following equation could be furthermore satisfied [87–89].

$$\| (A(N + \triangle N) - AN)M^{-1} \|_{Lip} < 1 \tag{2.17}$$

where $\| \cdot \|_{Lip}$ is a Lipschitz norm. Then the nonlinear feedback control system is robust stability. where M is an unimodular operator.

2.5 Impedance matching

In the 4-coil WPT systems with buck circuit as shown in Fig. 2.8, impedance matching can be used to obtain the high power transfer efficiency. Impedance matching is a popular scheme to track the desired equivalent load for coupling systems in WPT systems, thus high efficiency of the coupling system can be

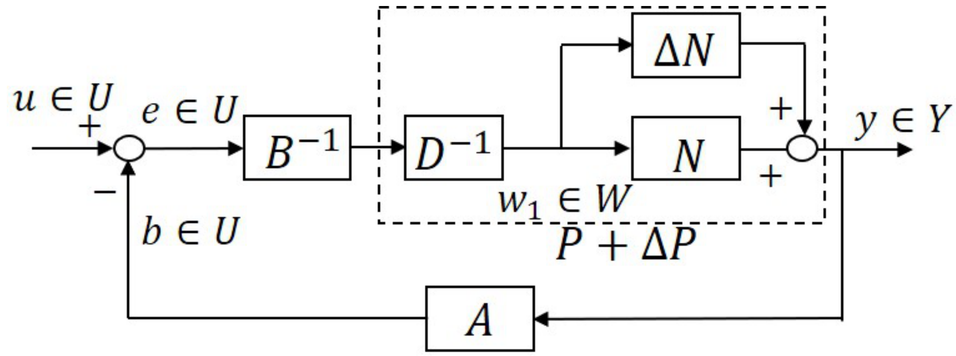

Figure 2.7: Feedback nonlinear system with uncertainties

obtained. The optimal equivalent load from load side to the receive side $R_{3L,opt}$ should satisfy the following equation.

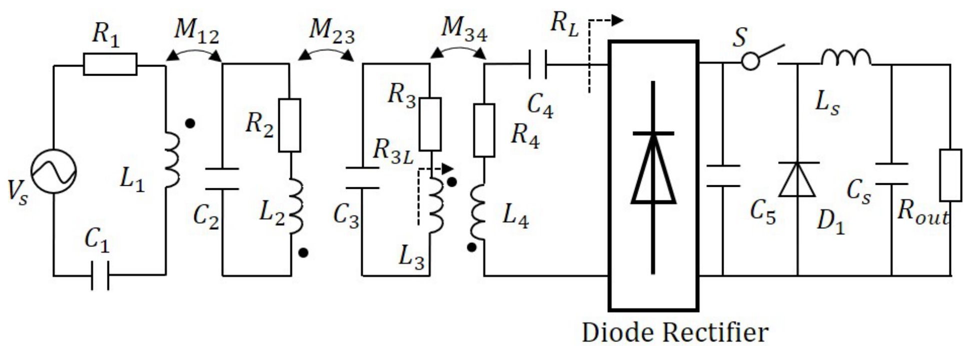

Figure 2.8: WPT system with buck circuit.

$$R_{3L,opt} = \frac{(wM_{34})^2}{R_{L,opt}} = R_3\sqrt{1 + \frac{(wM_{23})^2}{R_2 R_3}} \tag{2.18}$$

So $R_{L,opt}$ can be calculated as follows.

$$R_{L,opt} = \frac{(wM_{34})^2}{R_3\sqrt{1 + \frac{(wM_{23})^2}{R_2R_3}}} \tag{2.19}$$

The equation indicates that, if we let the positions of the coils fixed, then $R_{L,opt}$ can be calculated. It can also be observed that, by tuning D_3, the desired $R_{L,opt}$ can be obtained with a fixed R_{out}. Thus the corresponding optimal duty cycle $D_{3,opt}$ is

$$D_{3,opt} = \sqrt{\frac{8R_{out}}{\pi^2 R_{L,opt}}}. \tag{2.20}$$

2.6 Problem statement

In this dissertation, the WPT system with DC-DC circuits which is driven by the duty cycle of switch. The difficulty is to deal with the uncertain terms about the distance between coils (mutual inductance) and variation of output load in the nonlinear control design system. It is necessary to propose suitable closed-loop control schemes to realize the power management of the WPT system to tackle such problem.

Firstly, there are different closed-loop feedback control design schemes in WPT systems with DC-DC converters, such as PID control scheme, hysteresis method, perturbation-and-observation control scheme, and sliding mode control (SMC) method. The PID control scheme was proposed in a WPT system to track the reference signal, but the speed to track the reference signal is slow because the inherent shortage exists in traditional PID compensator. Hysteresis method is used in a WPT system with a boost circuit to realize the desired transfer power, but the stability of the WPT system have not been considered with the infinite frequency of a switch in practice.

Proportional and observations method is widely used in WPT system with buck circuit, boost circuit, and buck-boost circuit, the maximum efficiency and desired power could be obtain at the same time. However, the searching time is long and the settling transien period is needed. Also, SMC scheme is a promising way adopted in WPT system with DC-DC circuits because of the fast tracking speed and simple implementation. But the accurate distance between coils are difficult to achieved in the WPT experiments and the mutual inductance is very sensitive to the resonant coils' distance. Motivated by operator theory for uncertain nonlinear systems, to deal with the uncertain mutual inductance, which is caused by the inaccurate distance between the resonant coils in the WPT systems, a robust nonlinear control design scheme based on operator theory using sliding mode technology is given. By using the proposed control scheme, the robust stability of the WPT system with the uncertain term can be guaranteed. Besides, sliding mode technology can help to track the desired signal. Finally, the simulations and experiments are tested to confirm its effectiveness.

Secondly, the chattering phenomenon exists because of the inherent shortage of traditional SMC technology by using the method mentioned above. Motivated by the elimination method of chattering phenomenon existing in traditional SMC technology, the tracking performance could be improved by eliminating the chattering phenomenon. It is difficult to deal with the uncertain term and improve the tracking performance of output voltage at the same time. A proposed new nonlinear robust control design scheme based on operator theory for WPT systems with uncertainties is given. when the new proposed control design scheme is adopted, the robust stability can be guaranteed by using robust right coprime factorization approach. Moreover, the tracking performance is improved. Simulations and experiments are conducted to analyze the effectiveness of this proposed control design system.

Thirdly, the tracking performance of output voltage could be obtained for the robust WPT control system by using the above two proposed control schemes. But the impedance matching may be destroyed when the output load is varied, thus the high efficiency could not be maintained. Besides, the acquisition of AC signals with high frequency in previous researches would increase the complexity of the setup. Motivated by the power management of both transfer power and efficiency, not only the tracking performance of output voltage should be obtained, but also the impedance matching need to be realized to obtain high efficiency when the output load varies, and the acquisition of high frequency AC signal should be eliminated. Furthermore, the stability and robustness of the designed control systems need to be dealt with. So a proposed operator-based optimal equivalent load tracking control scheme is conducted for WPT systems with uncertain term. The robust stability of the feedback nonlinear system can be guaranteed by using robust right coprime factorization approach. Besides, the impedance matching of the WPT systems can be obtained without the acquisition of the AC signal, so high efficiency could be obtained and complexity of the setup is erased. Moreover, the constant output voltage could be obtained in the WPT system. Simulations are shown to verify that the proposed control design scheme is effectiveness.

In summary, the dissertation intends to propose three kinds of robust nonlinear design schemes based on operator theory for WPT systems.

2.7 Conclusion

In this chapter, the circuit theory of coupling systems, the modeling of buck circuit, the basic theories of operator-based control schemes and impedance matching are introduced. In addition, the problems which is discussed in this dissertation are stated, which gives the framework of our work.

Chapter 3

Operator-based robust nonlinear control of uncertain wireless power transfer (WPT) systems

3.1 Introduction

In this chapter, the setup of the WPT system is given and its corresponding mathematical modeling is derived and SMC method used in this proposed method is introduced. Then an operator-based robust nonlinear control design scheme is proposed to tackle the uncertain mutual inductance, which is resulting from the movement between resonant coils in WPT systems.

In Section 3.2, the derivation about the mathematical modeling of WPT systems is presented and the sliding mode control method is introduced.

In Section 3.3, based on the above modeling of the WPT system, an operator-based robust nonlinear control design scheme is proposed to tackle the uncertain mutual inductance, which is resulting from the movement distance between transmit coil and receive coil. The proposed control design method has two merits. Firstly, to deal with the uncertain term, the robust right coprime factorization approach is adopted to guarantee the robust stability of the uncertain WPT system. Then sliding mode technology is used to obtain the desired output voltage in the WPT system.

In Section 3.4, simulations and experiments are conducted to show the effectiveness of the proposed control design scheme.

In Section 3.5, the conclusion about the chapter is presented.

3.2 Modeling of the WPT system with a buck circuit and sliding mode control technology

3.2.1 Modeling of the WPT system with a buck circuit

The setup of the WPT system using a buck circuit is shown in Fig. 3.1, it includes the power source, the coupling system, the rectifying circuit, and the buck circuit. Besides, the sampling board is connected to the processing unit so that the WPT system is controllable. The proposed control method was conducted in a TMS320C6713 DSP embedded control system, the reason is that this type DSP has high digital signal processing capability and high operating frequency (the operation frequency could achieve $225MHz$).

The coupling system includes four parallel helical coils, and their position is shown in Fig. 3.2. O_1, O_2, O_3 and O_4 are the center of the four coils, respectively. O_1 is the origin of the coordinates in the three dimensional coordinates, i.e., $(0, 0, 0)$. In the setup, the relative position of the coils can be determined by the coordinates of O_2, O_3 and O_4.

The equivalent circuit of this WPT system can be shown in Fig. 3.3. The resonant loops are linked by the mutual inductances M_{12}, M_{23}, and M_{34}, which depends on the locations of the coils. V_s means power source, V_1 and f are the amplitude and frequency of V_s, respectively. R_s, L_1 and C_1

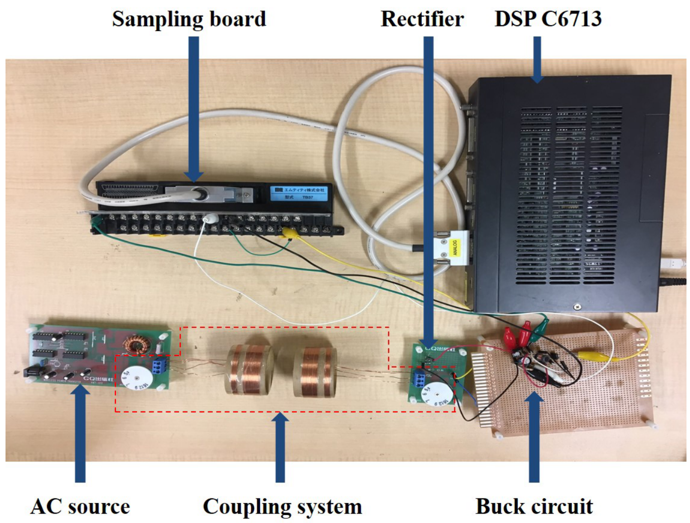

Figure 3.1: Setup of the WPT system.

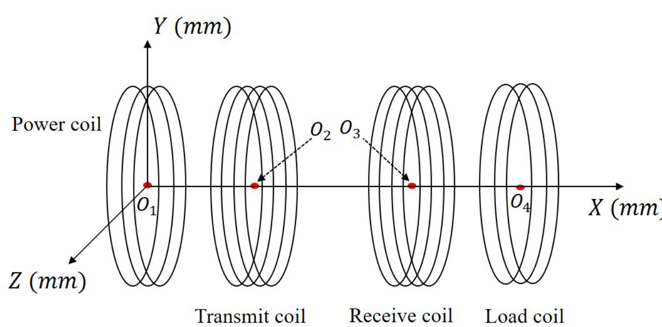

Figure 3.2: Relative position of the coils.

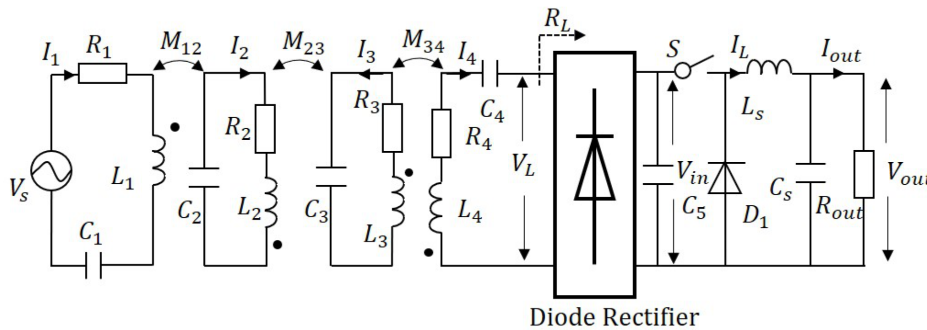

Figure 3.3: Equivalent circuit of the WPT system.

are the source resistance, inductor and compensated capacitor of the source coil. R_2, L_2 and C_2 are the parasitic resistance, inductor and compensated capacitor of the transmit loop. R_3, L_3 and C_3 are the parasitic resistance, inductor and compensated capacitor of the receive loop. R_4, L_4 and C_4 are the parasitic resistance, inductor and compensated capacitor of the load loop. C_5 is a big capacitor to stabilize the voltage, L_s and C_s are the filter inductor and the filter capacitor of the buck circuit, D_2 and S are the diode and switch of the buck circuit, R_{out} is the output resistance.

In Fig. 3.3, for simplicity, three assumptions are made as follows: 1. Only the first harmonic V_{ac} of V_L is considered. 2. The buck circuit in the WPT system is considered to be lossless. 3. C_5 can be used to stabilize V_{in}. Then let R_L be the equivalent load of both the rectifier and buck circuit, the mathematical modeling can be expressed by using Kirchhoff's voltage law as follows.

$$\begin{aligned}
I_1\left(R_s + jwL_1 + \frac{1}{jwC_1}\right) + jwI_2M_{12} = V_s\\
I_2\left(R_2 + jwL_2 + \frac{1}{jwC_2}\right) + jw\left(I_1M_{12} - I_3M_{23}\right) = 0\\
I_3\left(R_3 + jwL_3 + \frac{1}{jwC_3}\right) + jw\left(I_4M_{34} - I_2M_{23}\right) = 0\\
I_4\left(R_L + R_4 + jwL_4 + \frac{1}{jwC_4}\right) + jwI_3M_{34} = 0
\end{aligned} \tag{3.1}$$

where $w = 2\pi f$.

Then $V_{ac} = I_4R_L$ can be calculated by using the above four KVL equations, where $jwL_i = \frac{1}{jwC_i}(i = 1, 2, 3, 4)$

$$\begin{aligned}
V_{ac} &= \frac{jw^3M_{12}M_{23}M_{34}R_LV_s}{w^4M_{12}^2M_{34}^2 + Z_1Z_2Z_3Z_4 + w^2\kappa}\\
Z_1 &= R_s + jwL_1 + \frac{1}{jwC_1}\\
Z_2 &= R_2 + jwL_2 + \frac{1}{jwC_2}\\
Z_3 &= R_3 + jwL_3 + \frac{1}{jwC_3}\\
Z_4 &= R_L + R_4 + jwL_4 + \frac{1}{jwC_4}\\
\kappa &= M_{12}^2Z_3Z_4 + M_{23}^2Z_1Z_4 + M_{34}^2Z_1Z_2
\end{aligned} \tag{3.2}$$

Define and V_2 is the amplitude of V_{ac}, because the existence of capacitor C_5, the top value V_{L1} and the low value V_{L2} of the square waveform V_L can be obtained using the Fourier method.

$$V_{L1} = -V_{L2} = \frac{\pi}{4}V_2 \tag{3.3}$$

Then V_{in} can be calculated as follows.

$$V_{in} = V_{L1} = |V_{L2}| = \frac{\pi w^3M_{12}M_{23}M_{34}R_LV_1}{4\left(w^4M_{12}^2M_{34}^2 + Z_1Z_2Z_3Z_4 + w^2\kappa\right)} \tag{3.4}$$

It is worth mentioning that V_{in} includes the equivalent load R_L which have not been analysed.

Then our aim is to get R_L. With the above assumptions, the input signals to the rectifier includes an ideal sinusoidal current which is caused by the resonant components and a square wave voltage due to the stabilize capacitor. Define D_3 be the duty ratio of switch S ($D_3 = t_{on}/T$, t_{on} is the period during which S is on, and T is the time of one switching time). The expression about I_4 and I_{out}, the expression about V_{ac} and V_{out} can be got as follows.

$$\begin{aligned} I_4 &= \frac{\pi}{2} D_3 I_{out} sin\ \theta \\ V_{ac} &= \frac{4V_{out}}{\pi D_3} sin\ \theta \end{aligned} \tag{3.5}$$

Then R_L can be calculated as follows, and it can be observed from the equation that R_L is determined by D_3 even when R_{out} is fixed.

$$R_L = V_{ac}/I_4 = \frac{8R_{out}}{(\pi D_3)^2} \tag{3.6}$$

To take the transient response of the buck circuit into consideration, the modeling of the WPT system is as follows.

$$\begin{aligned} \frac{dI_L}{dt} &= \frac{1}{L_s}\left(D_3 V_{in} - V_{out}\right) \\ \frac{dV_{out}}{dt} &= \frac{1}{C_s}\left(I_L - \frac{V_{out}}{R_{out}}\right) \end{aligned} \tag{3.7}$$

For the simply expression of the mathematical modeling for the WPT system, we define the following functions.

$$\begin{aligned}
M_1 &= -\frac{1}{2R_{out}C_s} \\
N_1 &= \sqrt{\frac{1}{(2R_{out}C_s)^2} - \frac{1}{C_sL_s}} \\
X_1 &= M_1 + N_1 \\
Y_1 &= M_1 - N_1 \\
M_2 &= D_3V_{in}\frac{M_1 - N_1}{2N_1} \\
N_2 &= -D_3V_{in}\frac{M_1 + N_1}{2N_1}
\end{aligned} \tag{3.8}$$

So the mathematical plant P of the WPT system can be derived as the following equation with (3.6) and the expression about Z_4 and κ in (3.2).

$$V_{out} = M_2e^{X_1t} + N_2e^{Y_1t} + D_3V_{in} \tag{3.9}$$

where,

$$V_{in} = \frac{\pi w^3 M_{12}M_{23}M_{34}R_LV_1}{4\left(w^4M_{12}^2M_{34}^2 + Z_1Z_2Z_3Z_4 + w^2\kappa\right)} \tag{3.10}$$

and e means a euler constant. The plant is nonlinear because of the complex variable V_{in}, which is determined by the variable equivalent load R_L (D_3).

3.2.2 Calculation of the reference signal to obtain high efficiency

As discussed in Section 2.3, to obtain the high efficiency, the the optimal duty cycle $D_{3,opt}$ should be

$$D_{3,opt} = \sqrt{\frac{8R_{out}}{\pi^2R_{L,opt}}}. \tag{3.11}$$

So the optimal reference output voltage to achieve impedance matching can be obtained as follows.

$$V_{ref,1} = D_{3,opt}\frac{\pi w^3M_{12}M_{23}M_{34}R_{L,opt}V_1}{4\left(w^4M_{12}^2M_{34}^2 + Z_1Z_2Z_3Z_{4,opt} + w^2\kappa_{opt}\right)}. \tag{3.12}$$

3.2.3 Sliding mode control technology

In nonlinear systems, SMC provides a popular control method because of the short tracking time. When the sliding manifold and the control law for switch are properly designed, the states of the system will move to the sliding manifold and converge to the origion [72–76]. In application systems, the sliding function is always defined as follows.

$$S_1 = \alpha_1 e_1 + \dot{e}_1. \tag{3.13}$$

where $\alpha_1 > 0$, e_1 and $\dot{e}_1$ are the error between the transient value and desired value, the derivation of the error, respectively. Besides, to eliminate the chattering problem due to the finite frequency of switch in setup, hysteresis modulation (HM) was adopted as the control law, h is the hysteresis band of HM.

$$u = \begin{cases} 1 & when\ S_1 > +h \\ 0 & when\ S_1 < -h \end{cases} \tag{3.14}$$

3.3 Proposed operator-based robust nonlinear control scheme using sliding mode control technology

3.3.1 Proposed operator-based robust nonlinear control system design

Fig. 3.4 shows the proposed operator-based robust nonlinear control system for the WPT system.

The mathematical modeling P considering the uncertain term ΔP can be given for the WPT system as follows.

$$P + \Delta P: \quad y = (1+\Delta)\left(M_2 e^{X_1 t} + N_2 e^{Y_1 t} + D_3 V_{in}\right) \tag{3.15}$$

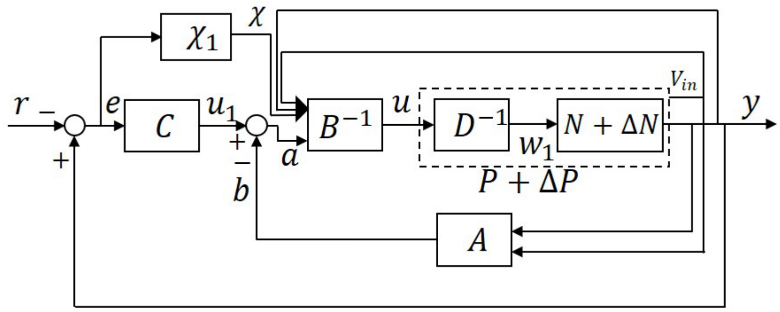

Figure 3.4: Proposed robust nonlinear control scheme.

where Δ is the uncertain term of the WPT system ($\|\Delta\| < 1$) resulting from the inaccurate distance between transmit coil and receive coil, y is the output voltage V_{out}, and V_{in} is a variable voltage.

The input control of switch S contains two states ($u = 0$ and $u = 1$) to decide whether the switch is on or off in simulations (Matlab/Simulink) and experiments. In this paper, $u = 1$ is used to close the switch and $u = 0$ is used to open the switch. Duty cycle D_3 represents the equivalent control of u ($0 < D_3 < 1$) and w_{eq} is the equivalent control of the quasi-state w_1. The plant can be right factorized as follows.

$$N + \Delta N : \quad y = (1+\Delta)\Big((1-w_{eq})\, V_{in} \frac{M_1 - N_1}{2N_1} e^{X_1 t} - (1-w_{eq}) \Big) \cdot V_{in} \frac{M_1 + N_1}{2N_1} e^{Y_1 t} + (1-w_{eq})\, V_{in} \tag{3.16}$$

$$D : \quad D_3 = 1 - w_{eq} \tag{3.17}$$

To analyse the stability, robust stability and tracking performance of the control system, we designed the compensators C and χ_1 using sliding mode technology as follows.

$$C : \quad u_1 = e_1 + K \tag{3.18}$$

$$\chi_1 : \quad \chi = \alpha e_1 + \dot{e}_1 + K \tag{3.19}$$

where K is a designed number satisfying $K > 1$, r is the reference signal V_{ref}, e_1 and α are

$$e_1 = y - r \tag{3.20}$$

$$\alpha = \frac{1}{R_{out}C_s} + 1. \tag{3.21}$$

The operator-based feedback control system is shown in Fig. 3.5. The operators A and B were designed as follows.

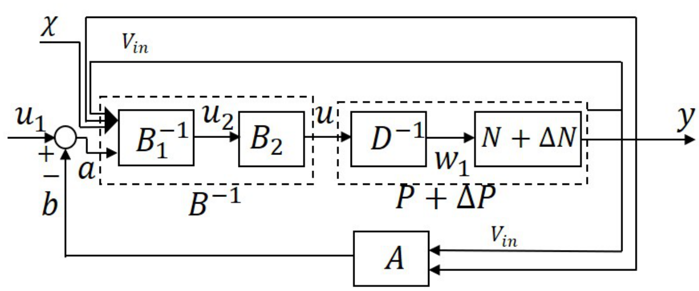

Figure 3.5: Operator-based feedback control system using sliding mode technology.

$$A: \quad b = 1 - \left[\frac{CL}{V_{in}}\left(\frac{d^2y}{dt^2} + \frac{y}{CL} + \frac{1}{R_{out}C}\frac{dy}{dt}\right)\right] \tag{3.22}$$

$$B^{-1}: \quad u = \frac{\mathbf{sgn}(a + 1 - D_3 - \chi) + 1}{2} \tag{3.23}$$

where **sgn** is the sign of the signal, it is worth mentioning that A is designed as the inverse function of N ($A = N^{-1}$). As shown in Fig. 3.5, the designed operator B^{-1} can also be expressed using $B_1^{-1} : a \rightarrow u_2$ and $B_2 : u_2 \rightarrow u$ as follows.

$$B_1^{-1}: \; u_2 = a + 1 - D_3 - \chi \tag{3.24}$$

$$B_2: \; u = \frac{\mathbf{sgn}(u_2) + 1}{2} \tag{3.25}$$

By using the proposed control design scheme, $e_1 = \dot{e}_1 = 0$ and $u_2 \to 0$ can be obtained to achieve the tracking performance when time comes to infinite. Besides, $w_{eq} = 1 - D_3$ $(0 < w_{eq} < 1)$ because of (3.17). As shown in Fig. 3.5, $a = BD(w_{eq}) = B_1(u_2)$. Besides, $A = N^{-1}$ and $B_1 : a = u_2 - 1 + D_3 + \chi$ using (3.24). Then by using the designed operators, $\tilde{M}$ in $A\,(N + \triangle N) + BD = \tilde{M}$ can be calculated as follows.

$$\begin{aligned}\tilde{M} &= (A(N + \Delta N) + BD)\,(w_{eq}) \\ &= A(N + \Delta N)(w_{eq}) + BD(w_{eq}) \\ &= (1 + \Delta)N^{-1}N(w_{eq}) + B_1(u_2) \\ &= w_{eq} + \Delta \cdot w_{eq} + u_2 - 1 + D_3 + \chi \\ &= w_{eq} + \Delta \cdot w_{eq} + u_2 - 1 + D_3 + \alpha e + \dot{e} + K \\ &= K + \Delta \cdot w_{eq}.\end{aligned} \tag{3.26}$$

$\tilde{M}$ is an unimodular operator because $K > 1$, $\|\Delta\| < 1$ and $0 < w_{eq} < 1$. M is the simplified operator of $\tilde{M}$ without the uncertain term Δ, so $M = K$.

Moreover, the Lipschitz norm of $\left\|[A\,(N + \Delta N) - AN]M^{-1}\right\|_{Lip}$ could be calculated as follows.

$$\begin{aligned}&\|[A\,(N + \Delta N) - AN]M^{-1}\|_{Lip} \\ \leq\ &\|A\,(N + \Delta N) - AN\|_{Lip} \cdot \|M^{-1}\| \\ =\ &\|A\Delta N\|_{Lip} \cdot \frac{1}{K} \\ =\ &\|\Delta\| \cdot w_{eq} \cdot \frac{1}{K} \\ <\ &1\end{aligned} \tag{3.27}$$

So the feedback control system is robust stability.

3.3.2 Proposed tracking control design

Because the direct implementation of **sgn**() in (3.23) will cause the WPT system to operate at an uncontrollable infinite switching frequency which is not desire in practice. Therefore, HM method is employed with a hysteresis band h in proposed tracking control system to solve the high frequency operation, thus guaranteeing the tracking performance. The HM method is designed as follows.

$$u = \begin{cases} 1 & when\ u_2 > +h \\ 0 & when\ u_2 < -h \end{cases}$$

The proposed tracking control system is designed as shown in Fig. 3.6.

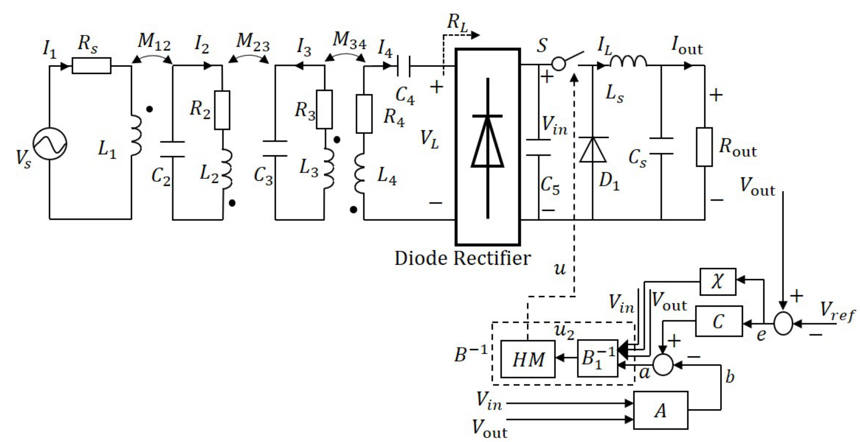

Figure 3.6: Proposed tracking control system.

As shown in Fig. 3.4, $a = u_1 - b$. Besides, $w_{eq} = 1 - D_3$ has been illustrated. With the designed compensators $C : u_1 = e + K$ and $\chi_1 : \chi = \alpha e + \dot{e} + K$. Then the calculation of u_2 can be expressed as follows.

$$\begin{aligned} u_2 &= a + 1 - D_3 - \chi \\ &= (u_1 - b) + 1 - D_3 - (\alpha e_1 + \dot{e}_1 + K) \\ &= e + K - w_{eq} + 1 - D_3 - (\alpha e_1 + \dot{e}_1) - K \\ &= -(\alpha - 1)e_1 - \dot{e}_1 \end{aligned} \tag{3.28}$$

The time derivative of u_2 is

$$\dot{u}_2 = -(\alpha - 1)\dot{e}_1 - \ddot{e}_1. \tag{3.29}$$

Define $x_1 = e_1(t)$ and $x_2 = \dot{e}_1(t)$. The modeling of N of the WPT system can be obtained as follows using (3.17) and (3.20), (3.7).

$$\begin{aligned} \dot{x}_1 &= x_2 \\ \dot{x}_2 &= -\frac{\dot{x}_1}{R_{out}C_s} + \frac{1}{L_sC_s}\Big[\big(1 - w_{eq}\big)V_{in} - V_{ref} - x_1\Big] \end{aligned} \tag{3.30}$$

Because of the inherent property of the buck circuit in the WPT system, V_{out} is less than V_{in}. The following equations can be obtained using (3.20), (3.21), (3.25), (3.29) and (3.30).

$$\begin{aligned} \dot{u}_2 &= -\frac{1}{L_sC_s}\left(V_{in} - V_{ref} - e_1\right) < 0 \quad u_2 > 0 \\ \dot{u}_2 &= \frac{1}{L_sC_s}\left(V_{ref} + e_1\right) > 0 \qquad\qquad u_2 < 0 \end{aligned} \tag{3.31}$$

Because of (3.31), as time goes, u_2 satisfies the following equations.

$$\begin{aligned} u_2 &= -(\alpha - 1)e_1 - \dot{e}_1 = 0 \\ \dot{u}_2 &= -\frac{1}{L_sC_s}\big[(1 - w_{eq})V_{in} - V_{ref} - e_1\big] = 0 \end{aligned} \tag{3.32}$$

Thus w_{eq} can be obtained as

$$w_{eq} = 1 - \frac{V_{ref} - e_1\left(0\right)e^{-\frac{t}{R_{out}C_s}}}{V_{in}}. \tag{3.33}$$

where $e(0)$ is the value of e at $t = 0$.

In the WPT system, parameters X_1, Y_1, and $-1/(R_{out}C_s)$ are negative numbers. As $t \to \infty$,

$$\begin{aligned} &e^{X_1 t} \to 0 \\ &e^{Y_1 t} \to 0 \\ &e^{-\frac{t}{R_{out}C_s}} \to 0. \end{aligned} \tag{3.34}$$

Then y in steady state ($t \to \infty$) can be obtained as follows.

$$\begin{aligned} y =& N(w_{eq}) \\ =& (1-w_{eq})\, V_{in}\frac{M_1-N_1}{2N_1}e^{X_1 t}-(1-w_{eq}) \\ & \cdot V_{in}\frac{M_1+N_1}{2N_1}e^{Y_1 t}+(1-w_{eq})\, V_{in} \\ \to& \Big[1-\big(1-\frac{V_{ref}-e_1(0)e^{-\frac{t}{R_{out}C_s}}}{V_{in}}\big)\Big]V_{in} \\ \to& V_{ref}-e_1(0)e^{-\frac{t}{R_{out}C_s}} \\ \to& V_{ref} \end{aligned} \tag{3.35}$$

Therefore, the tracking performance is obtained ($e_1 = \dot{e}_1 = 0$).

From the discussion above, the robust stability can be guaranteed using robust right coprime factorization approach to deal with the uncertain distance (mutual inductance M_{23}) in the WPT system. Also, the tracking performance can be obtained using sliding mode technology.

3.4 Simulations and experiments

In order to confirm the effectiveness of the proposed operator-based robust nonlinear control design scheme, the WPT system with the buck circuit has been conducted both by simulations and experiments. The specifications of the WPT system are given in Table 3.1.

3.4.1 Simulations

When $M_{12} = M_{34} = 8.5\ \mu H$ and $M_{23} = 7.5\ \mu H$, to obtain the high power transfer efficiency, the reference signal is set as 2.46 V. The parameters of the proposed control design scheme are set as $h = 0.02$, $\alpha = 14$, $K = 1.4$. Simulations are carried out using the Simulink of Matlab with a small step size of 10 ns.

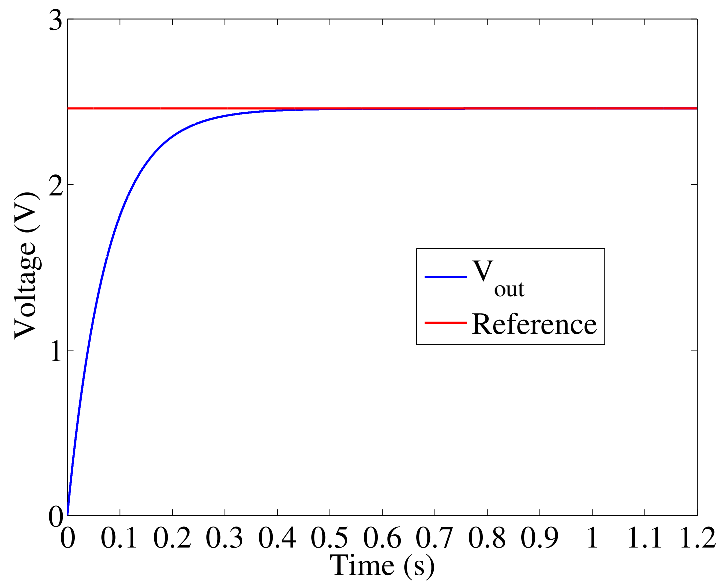

Figure 3.7: Output voltage of the WPT system with the certain term M_{23}.

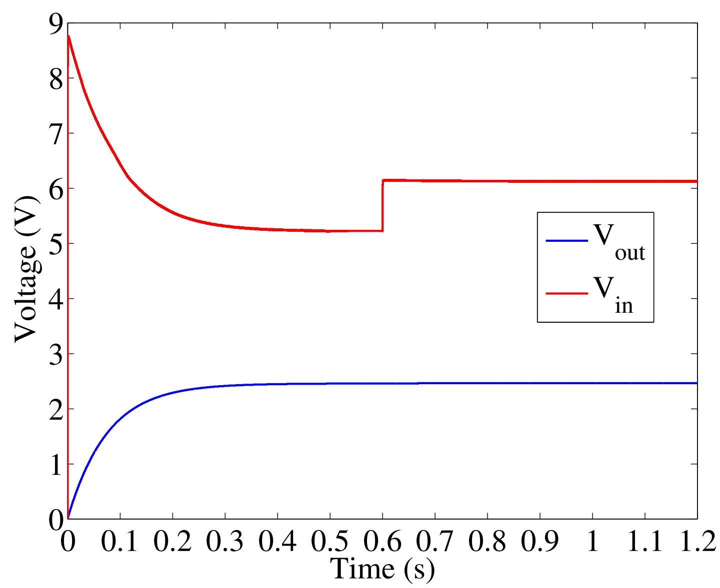

Figure 3.8: Output voltage of rectifying circuit and output voltage of the WPT system when M_{23} becomes larger than before at $t = 0.6$ s.

Table 3.1: Specifications of the WPT system.

Description	Parameter	Value	Unit
Amplitude of source voltage	V_1	12	V
Source frequency	f	2	MHz
Resistance in power loop	R_s	50	Ω
Transmit/Receive inductor	L_1, L_4	4.3	μH
Resonant inductors	L_2, L_3	35.3	μH
Resonant capacitors	C_2, C_3	179	pF
	C_1, C_4	1	nF
Parasitic resistance	R_2, R_3	45	Ω
	R_4	0.3	Ω
Large capacitor	C_5	1	μF
Filter capacitor	C_s	1000	μF
Filter inductor	L_s	1	mH
Output load	R_{out}	75	Ω

By using this proposed control method, Fig. 3.7 indicates that the output voltage V_{out} can track the reference signal 2.46 V with the certain term $M_{23} = 7.5\ \mu H$.

To consider the uncertain mutual inductance, when M_{23} changes from 7.5 μH to 9 μH (M_{23} becomes larger than before) at $t = 0.6\ s$, V_{in} and V_{out} can be obtained as shown in Fig. 3.8. When M_{23} changes from 7.5 μH to 7 μH (M_{23} becomes smaller than before) at $t = 0.6\ s$, V_{in} and V_{out} can be obtained as shown in Fig. 3.9.

It can be observed from Figs. 3.8 and 3.9, the output voltage can maintain the tracking performance even when there exists the uncertain term M_{23} (no matter M_{23} is larger or smaller than the normal value).

The Lipschitz norm $\|[A(N + \Delta N) - AN]M^{-1}\|_{Lip}$ is shown in Fig. 3.10. The maximum value is less than 1. Therefore, the robust stability is guaranteed using robust right coprime factorization.

Noted that, the input power is 450 mW, the output power is 81 mW, so

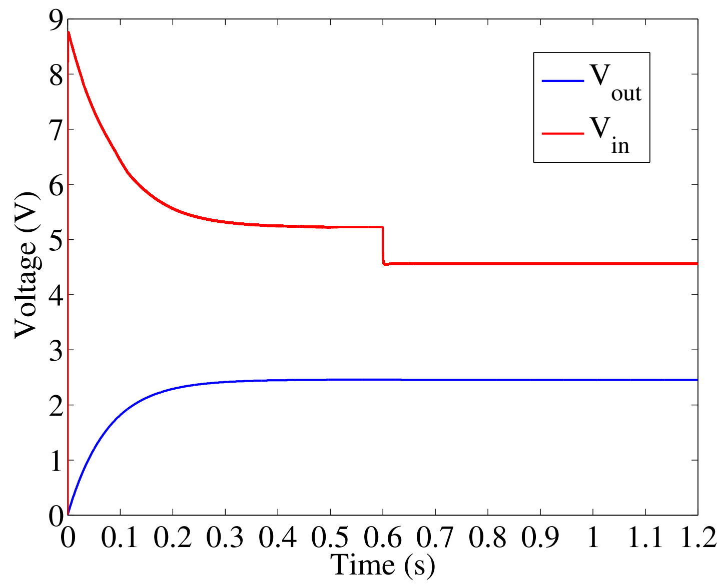

Figure 3.9: Output voltage of rectifying circuit and output voltage of the WPT system when M_{23} becomes smaller than before at $t = 0.6$ s.

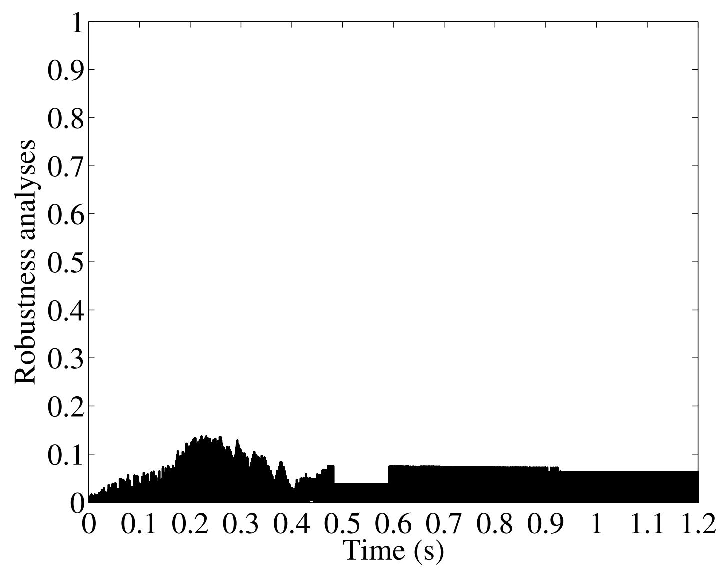

Figure 3.10: Robustness analyses.

the transfer efficiency is 17.6 % in this WPT system.

3.4.2 Experiments

In the setup, O_2, O_3 and O_4 are located at $(16, 0, 0)$, $(66, 0, 0)$ and $(82, 0, 0)$ to get $M_{12} = M_{34} = 8.5\ \mu H$ and $M_{23} = 7.5\ \mu H$. The reference signal and the parameters of the proposed control scheme were designed as same as those in simulations. The switching frequency of S is 20 KHz in the experiments.

The reference voltage is 2.46 V, when the coils are located at the positions as above (normal distance), the output voltage is shown in Fig. 3.11. It can be observed that the output voltage can track the reference voltage.

To consider the uncertain distance, when the position of O_3 and O_4 moves to $(56, 0, 0)$ and $(72, 0, 0)$ (the distance between O_2 and O_3 becomes smaller than before), respectively. V_{in} and V_{out} obtained in the experiments are shown in Fig. 3.12. When the position of O_3 and O_4 moves to $(71, 0, 0)$ and $(87, 0, 0)$ (the distance between O_2 and O_3 becomes larger than before), respectively. V_{in} and V_{out} obtained in the experiments are shown in Fig. 3.13. Noted that the green one represents V_{in} and the yellow one represents V_{out}.

When the distance between transmit coil and receive coil becomes smaller (uncertain distance) than the normal distance, the input voltage to rectifier and output voltage are shown in Fig. 3.12, and the two signals are shown in Fig. 3.13 when the distance between transmit coil and receive coil becomes larger (uncertain distance) than normal distance. It can be deduced from Fig. 3.12 and Fig. 3.13, the proposed control design scheme can always track the reference signal even when there exists a inaccurate distance in the WPT system.

From the above results about simulations and experiments, by using the proposed operator-based robust nonlinear control design scheme, the robust stability was guaranteed to tackle the uncertain distance (M_{23}), and the tracking performance can always be obtained in the WPT system.

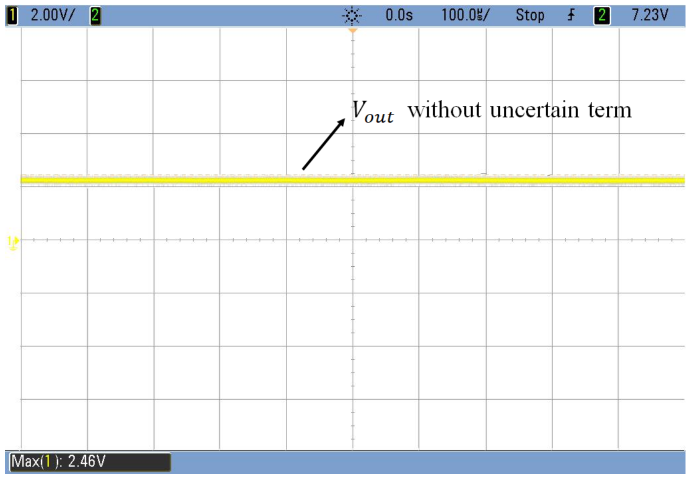

Figure 3.11: Output voltage of the WPT system with the certain distance.

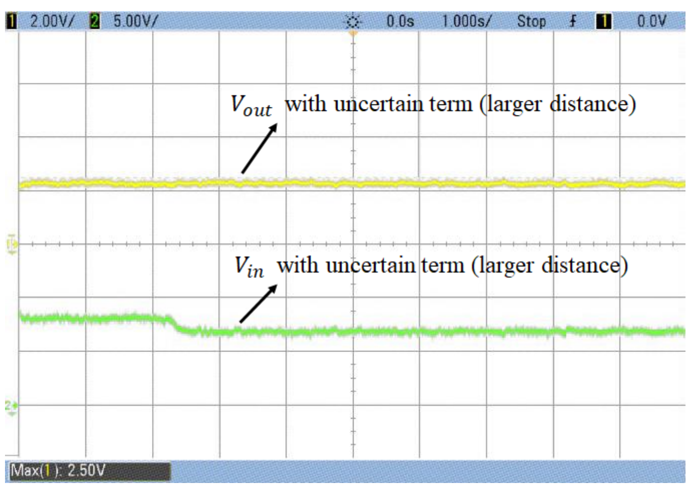

Figure 3.12: Output voltage of rectifying circuit and output voltage of the WPT system when the distance between transmit coil and receive coil becomes smaller than before.

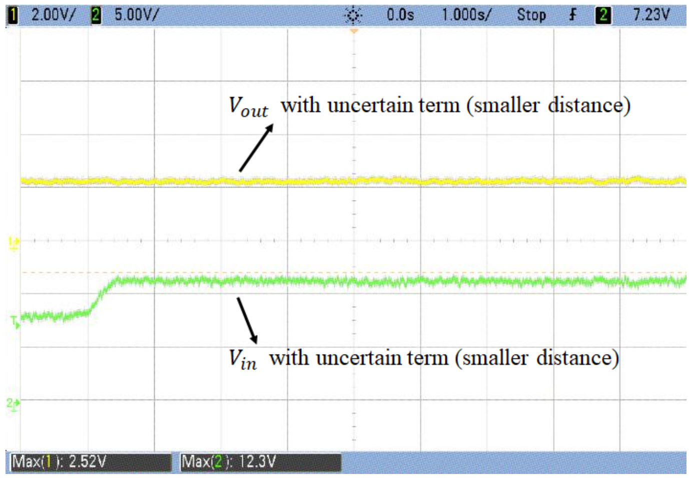

Figure 3.13: Output voltage of rectifying circuit and output voltage of the WPT system when the distance between transmit coil and receive coil becomes larger than before.

Noted that, the input power is 809 mW, the output power is 81 mW, so the transfer efficiency is 10 % in this WPT system due to the power loss on the DC-DC circuit (359 mW).

Besides, to analyses different align of the coils, when the transmit coil and receive coil are located as Fig. 3.14. To obtain the desired output voltage, when $x = 55$ mm, y should be 0 mm; when $x = 45$ mm, the range of y can achieve 17 mm; when $x = 35$ mm, the range of y can achieve 22 mm; when $x = 23$ mm, the range of y can achieve 31 mm.

3.5 Conclusion

In this chapter, to deal with the uncertain mutual inductance resulting from the inaccurate distance between transmit coil and receive coil in the WPT system, an operator-based robust nonlinear control design scheme using sliding mode technology was proposed. The proposed control design scheme can

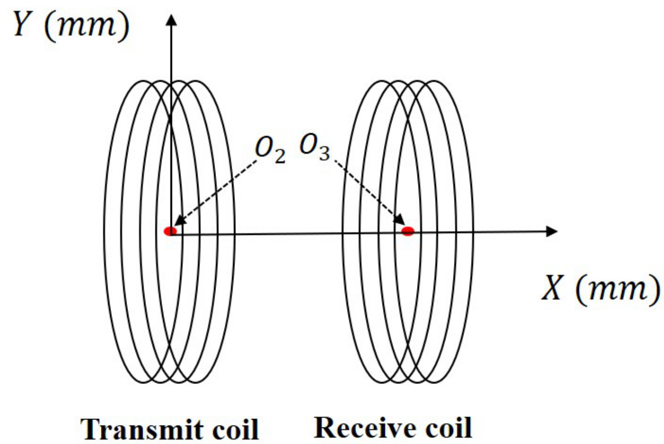

Figure 3.14: Relative position of the transmit coil and receive coil.

guarantee the robust stability of the WPT system with the uncertain term. Meantime, the tracking performance was also obtained by using sliding mode control method. The results of simulations and experiments were presented to confirm its effectiveness.

Chapter 4

Tracking performance improvement for operator-based robust nonlinear control of WPT systems with uncertainties

4.1 Introduction

In this chapter, the terminal sliding mode control method is introduced. Then a new proposed robust control design scheme for wireless power transfer systems with uncertainties is proposed based on operator theory. In the proposed control design system, to deal with the uncertainties in the wireless power transfer system, operator-based robust right coprime factorization approach is adopted to guarantee the robust stability. Moreover, the tracking performance can be improved when the proposed control design scheme is adopted.

In Section 4.2, the terminal SMC method is introduced.

In Section 4.3, a proposed robust control design scheme for WPT systems with uncertainties is proposed based on operator theory, where, from different viewpoint, the considered nonlinear system is of Input/Output presentation. The robust stability could be guaranteed by using operator-based robust right coprime factorization approach.

In Section 4.4, simulations and experiments are conducted to confirm the effectiveness of the new operator-based nonlinear robust control design scheme.

In Section 4.5, the conclusion is presented.

4.2 Terminal sliding mode control method

For a nonlinear system as follows, the TSM manifold for the system can be designed in the following form.

$$s = \ddot{e}_1 + \mathit{\Gamma}_1 \dot{e}_1^{\alpha_2} + \mathit{\Gamma}_2 e_1^{\alpha_1} \tag{4.1}$$

where e_1 is the system state, $\mathit{\Gamma}_i$ and α_i $(i = 1, 2)$ are the designed parameters in TSM manifold. To obtain the tracking performance, $\mathit{\Gamma}_i$ should be determined to guarantee that the polynomial $p^2 + \mathit{\Gamma}_1 p + \mathit{\Gamma}_2$ is Hurwitz, thus all the eigenvalues of the polynomial are negative. Besides, α_i should be designed based on the following equations and $0 < \alpha_i < 1$.

$$\alpha_1 = \alpha_2/(2 - \alpha_2) \tag{4.2}$$

Once the ideal sliding mode $s = 0$ could be maintained, the nonlinear system will behave as follows.

$$\ddot{e}_1 + \mathit{\Gamma}_1 \dot{e}_1^{\alpha_2} + \mathit{\Gamma}_2 e_1^{\alpha_1} = 0 \tag{4.3}$$

Noted that when SM manifold ($s = \ddot{e}_1 + \mathit{\Gamma}_1 \dot{e}_1 + \mathit{\Gamma}_2 e_1$) is adopted, the system will converge to its equilibrium point along SM manifold in infinite time if $\mathit{\Gamma}_i$ are selected to guarantee that the polynomial $p^2 + \mathit{\Gamma}_1 p + \mathit{\Gamma}_2$ is Hurwitz. When TSM manifold is adopted, α_i in (4.1) are also adopted and determined using (4.2), system (4.3) can converge to its equilibrium point from any initial condition along the TSM manifold in finite time [90–95].

4.3 New operator-based nonlinear robust control design scheme

In the subsection, the proposed new nonlinear robust control design scheme is shown in Fig. 4.1, and the operators C, χ, F_1, B_1^{-1}, B_2 and F_2 are as follows.

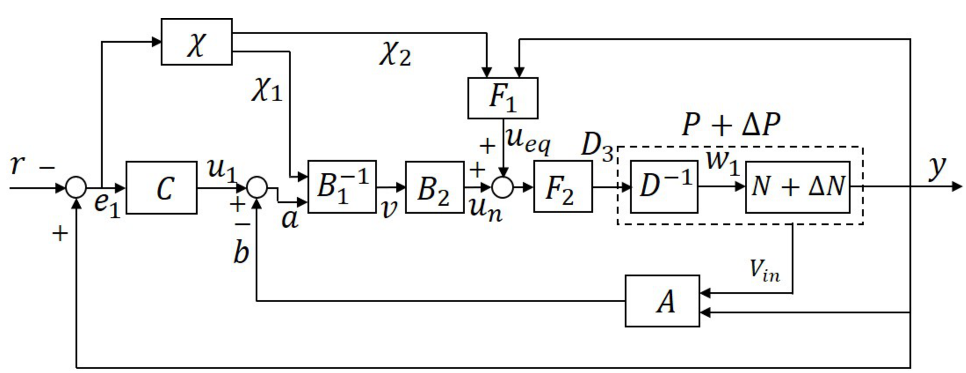

Figure 4.1: Proposed operator-based nonlinear robust control design scheme.

$$C: \quad u_1 = K_1 e_1^{\alpha_1} + K_2 \tag{4.4}$$

$$\chi: \quad \begin{array}{l} \chi_1 = \ddot{e}_1 + \mathit{\Gamma}_1 \dot{e}_1^{\alpha_2} + \mathit{\Gamma}_2 e_1^{\alpha_1} + K_2 \\ \chi_2 = \mathit{\Gamma}_1 \dot{e}_1^{\alpha_2} + (\mathit{\Gamma}_2 + K_1) e_1^{\alpha_1} \end{array} \tag{4.5}$$

$$F_1: \; u_{eq} = -\chi_2 + \frac{y}{L_s C_s} + \frac{\dot{y}}{R_{out} C_s} \tag{4.6}$$

$$A: \quad b = 1 - \Big[\frac{L_s C_s}{V_{in}}\big(\frac{d^2 y}{dt^2} + \frac{y}{L_s C_s} + \frac{1}{R_{out} C_s}\frac{dy}{dt}\big)\Big] \tag{4.7}$$

$$B_1^{-1}: \quad v = K_3 \cdot \mathbf{sgn}(a + 1 - D_3 - \chi_1) \tag{4.8}$$

$$B_2: \quad \dot{u}_n + T u_n = v \tag{4.9}$$

$$F_2: \quad D_3 = \frac{L_s C_s}{V_{in}}(u_{eq} + u_n) \tag{4.10}$$

where K_1, K_2, K_3, $\mathit{\Gamma}_1$, $\mathit{\Gamma}_2$, α_1, α_2 and T are designed parameters, satisfying $K_1 > 0$, $K_2 > 1$, $K_3 > 0$, $\mathit{\Gamma}_1^2 - 4(\mathit{\Gamma}_2 + K_1) > 0$, $\alpha_1 = \alpha_2/(2-\alpha_2)$, $0 < \alpha_i < 1$, $T > 0$ and $u_n(0) = 0$. **sgn** is the sign of the signal, $y = V_{out}$, $r = V_{ref}$, and $e_1 = y - r$.

In this proposed control design system, B_1^{-1} and B_2 are designed to eliminate the existence of **sgn** function in u_n, F_1 and F_2 are proposed to provide the input D_3 for the plant in which the chattering problem has been tackled. Then A is proposed to deal with the uncertain term of the WPT systems, compensators C and χ are designed to obtain the tracking performance.

4.3.1 Proposed operator-based robust control of the WPT system

The mathematical plant $P + \Delta P$ considering the uncertain term can be obtained as the following equation.

$$P + \Delta P: \quad y = (1 + \Delta)\left(M_2 e^{X_1 t} + N_2 e^{Y_1 t} + D_3 V_{in}\right) \tag{4.11}$$

where ΔP is the uncertain term of the WPT system. Since there exists the additive uncertainty in (4.11), as a result, we assume $\|\Delta\| < 1$, note that this assumption is realistic in WPT systems by limiting the uncertain distance between the resonance components.

The operator-based robust feedback control system is shown in Fig. 4.2.

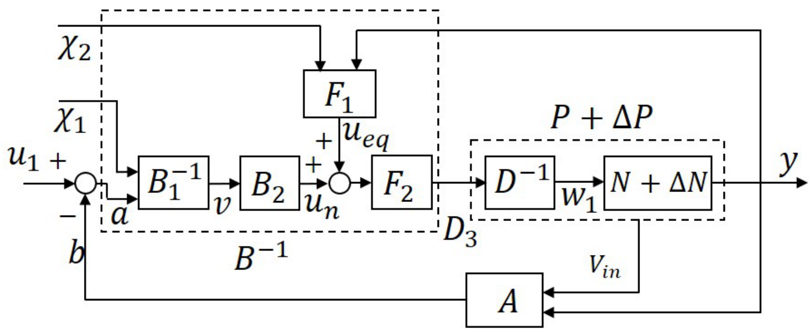

Figure 4.2: Proposed operator-based robust feedback control system.

The plant can be right factorized as follows.

$$\begin{aligned} N+\Delta N: \quad y =& (1+\Delta)\Big(\, (1-w_1)\, V_{in} \frac{M_1 - N_1}{2N_1} e^{X_1 t} \\ & - (1-w_1)\,\Big) \cdot V_{in} \frac{M_1 + N_1}{2N_1} e^{Y_1 t} \\ & + (1-w_1)\, V_{in} \end{aligned} \tag{4.12}$$

$$D: \quad D_3 = 1 - w_1 \tag{4.13}$$

It should be noted that A is designed as the inverse function of N ($A = N^{-1}$). Besides, $w_1 = 1 - D_3$ according to (4.13). By using the proposed control system design, we could obtain $e_1 = \dot{e}_1 = \ddot{e}_1 = 0$ and $v = 0$ to obtain the tracking performance when the control system is in the steady-state, which will be presented later. It also could be observed from Fig. 4.2 that $a = B_1[B_2^{-1}(F_2^{-1}(D_3) - F_1(\chi_2, y))] = B_1 v = \mathbf{sgn}^{-1}(v/K_3) + D_3 - 1 + \chi_1$. So $\tilde{M}$ in $A\,(N + \triangle N) + BD = \tilde{M}$ can be calculated as follows by using the designed parameters.

$$\begin{aligned}\tilde{M} =& \left(A(N+\Delta N)+BD\right)(w_1)\\ =& A(N+\Delta N)(w_1)+BD(w_1)\\ =& (1+\Delta)N^{-1}N(w_1)+B_1(v)\\ =& w_1+\Delta\cdot w_1+\mathbf{sgn}^{-1}(v/K_3)+D_3-1+\ddot{e}_1\\ &+\mathit{\Gamma}_1\dot{e}_1^{\alpha_2}+\mathit{\Gamma}_2 e_1^{\alpha_1}+K_2\\ =& K_2+\Delta\cdot w_1\end{aligned} \tag{4.14}$$

It could be deduced that $\tilde{M}$ is an unimodular operator, because $K_2 > 1$, $\|\Delta\| < 1$ and $0 < w_1 < 1$. By the way, M can be obtained as $M = K_2$ without uncertain term ($\Delta = 0$).

Furthermore, the Lipschitz norm of $\left\|[A\left(N+\Delta N\right)-AN]M^{-1}\right\|_{Lip}$ could be calculated as follows.

$$\begin{aligned}&\|[A\left(N+\Delta N\right)-AN]M^{-1}\|_{Lip}\\ \leq& \|A\left(N+\Delta N\right)-AN\|_{Lip}\cdot\|M^{-1}\|\\ =& \|A\Delta N\|_{Lip}\cdot\frac{1}{K_2}\\ =& \|\Delta\|\cdot w_1\cdot\frac{1}{K_2}\\ <& 1\end{aligned} \tag{4.15}$$

So the feedback control system is robust stability.

4.3.2 Proposed tracking control design system

The proposed control design scheme is shown in Fig. 4.1, $a = u_1 - b$ could be obtained. Besides, $w_1 = 1 - D_3$ by using (4.13). Define $s_1 = \ddot{e}_1 + \mathit{\Gamma}_1\dot{e}_1^{\alpha_2} + (\mathit{\Gamma}_2 + K_1)e_1^{\alpha_1}$ and $v_1 = a + 1 - D_3 - \chi_1$. With the designed compensator and operators, the relationship between v_1 and s_1 is

$$
\begin{aligned}
v_1 =& a + 1 - D_3 - \chi_1 \\
=& (u_1 - b) + 1 - D_3 - (\ddot{e}_1 + \mathit{\Gamma}_1 \dot{e}_1^{\alpha_2} + \mathit{\Gamma}_2 e_1^{\alpha_1} + K_2) \\
=& (e_1 + K_2 - w_1) + 1 - D_3 + (\ddot{e}_1 + \mathit{\Gamma}_1 \dot{e}_1^{\alpha_2} \\
& + \mathit{\Gamma}_2 e_1^{\alpha_1} + K_2) \\
=& - \ddot{e}_1 - \mathit{\Gamma}_1 \dot{e}_1^{\alpha_2} - (\mathit{\Gamma}_2 + K_1) e_1^{\alpha_1} \\
=& - s_1.
\end{aligned}
\tag{4.16}
$$

The modeling of the WPT system could be written as follows.

$$
\begin{aligned}
s_1 =& \ddot{e}_1 + \mathit{\Gamma}_1 \dot{e}_1^{\alpha_2} + (\mathit{\Gamma}_2 + K_1) e_1^{\alpha_1} \\
=& - \frac{\dot{e}_1}{R_{out} C_s} - \frac{y}{L_s C_s} + \frac{D_3 V_{in}}{L_s C_s} + \mathit{\Gamma}_1 \dot{e}_1^{\alpha_2} + (\mathit{\Gamma}_2 + K_1) e_1^{\alpha_1} \\
=& - \frac{\dot{e}_1}{R_{out} C_s} - \frac{y}{L_s C_s} + u_{eq} + u_n + \mathit{\Gamma}_1 \dot{e}_1^{\alpha_2} \\
& + (\mathit{\Gamma}_2 + K_1) e_1^{\alpha_1} \\
=& - \frac{\dot{e}_1}{R_{out} C_s} - \frac{y}{L_s C_s} - \chi_2 + \frac{y}{L_s C_s} + \frac{\dot{y}}{R_{out} C_s} \\
& + u_n + \mathit{\Gamma}_1 \dot{e}_1^{\alpha_2} + (\mathit{\Gamma}_2 + K_1) e_1^{\alpha_1} \\
=& - \chi_2 + u_n + \mathit{\Gamma}_1 \dot{e}_1^{\alpha_2} + (\mathit{\Gamma}_2 + K_1) e_1^{\alpha_1} \\
=& u_n
\end{aligned}
\tag{4.17}
$$

By using (4.9), the derivation of s_1 is

$$
\begin{aligned}
\dot{s}_1 &= \dot{u}_n \\
&= -T u_n + K_3 \cdot \mathbf{sgn}(v_1) \\
&= -T u_n - K_3 \cdot \mathbf{sgn}(s_1).
\end{aligned}
\tag{4.18}
$$

Hence

$$
\begin{aligned}
s_1 \cdot \dot{s}_1 &= s_1 \left(-T s_1 - K_3 \cdot \mathbf{sgn}(s_1) \right) \\
&= -T s_1^2 - K_3 \mid s_1 \mid \\
&< 0.
\end{aligned}
\tag{4.19}
$$

So the nonlinear system could reach to $s_1 = 0$ in finite time and stay on the manifold afterwards due to $s_1 \cdot \dot{s}_1 < 0$. Then the nonlinear system will behave as follows.

$$\ddot{e}_1 + \Gamma_1 \dot{e}_1^{\alpha_2} + (\Gamma_2 + K_1) e_1^{\alpha_1} = 0 \tag{4.20}$$

On $s_1 = 0$, because the parameters Γ_1, Γ_2, and K_1 satisfy $\Gamma_1^2 - 4(\Gamma_2 + K_1) > 0$, and α_1 and α_2 are designed satisfying (4.2) as designed before. The system (4.20) will be convergence to zero in finite time along $s_1 = 0$, thus the tracking performance can be obtained when the proposed tracking control design system is adopted ($e_1 = \dot{e}_1 = \ddot{e}_1 = 0$). Moreover, it is worthy mentioning that only v in (4.8) contains switching terms in the control system, while the actual control signal D_3 does not contain these terms, so chattering phenomenon is avoided.

Therefore, the robust stability could be guaranteed by using proposed operator-based nonlinear robust control design scheme. Moreover, the tracking performance could be obtained without chattering phenomenon, so the tracking performance is improved by using the new operator-based nonlinear robust control design scheme.

4.4 Simulations and experiments

To validate the effectiveness of the tracking performance improvement for operator-based nonlinear robust control design system, simulations and experiments are conducted by using the proposed control system. The block diagram for the control system with the proposed control design scheme is depicted in Fig. 4.3, besides, the period of the switching time is $5 * 10^{-5}s$.

The parameters of the proposed control scheme are designed as $V_{ref} = 2.5V$, $K_1 = 1$, $K_2 = 1.32$, $K_3 = 10$, $\Gamma_1 = 7$, $\Gamma_2 = 9$, $\alpha_1 = 9/23$, $\alpha_2 = 9/16$, and $T = 0.1$. In the designed parameters, the reference signal is set as $2.5V$;

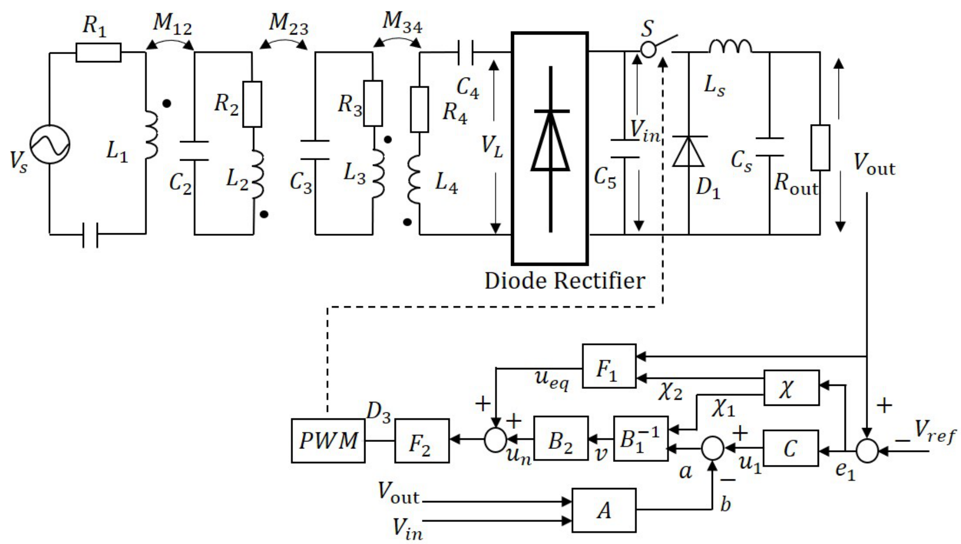

Figure 4.3: Proposed WPT system by using the proposed control design scheme.

$K_1 = 1$, $\Gamma_1 = 7$, and $\Gamma_2 = 9$ are designed satisfying $\Gamma_1^2 - 4(\Gamma_2 + K_1) > 0$ so that the system could converge to equilibrium point; K_2 is designed to be bigger than 1 so that the robust stability could be guaranteed; $\alpha_1 = 9/23$, $\alpha_2 = 9/16$ are proposed to obtain the finite time stable; then $K_3 = 10$ and $T = 0.1$ are selected to remove the chattering problem in traditional SM method.

4.4.1 Simulations

Improved tracking performance

The system states $x_1 = e_1$ and $x_2 = \dot{e}_1$ using the previous method and proposed method are shown in Figs. 4.4 and 4.5, respectively. Besides, the actual control input of the control system is depicted in Fig. 4.6 by using the two methods.

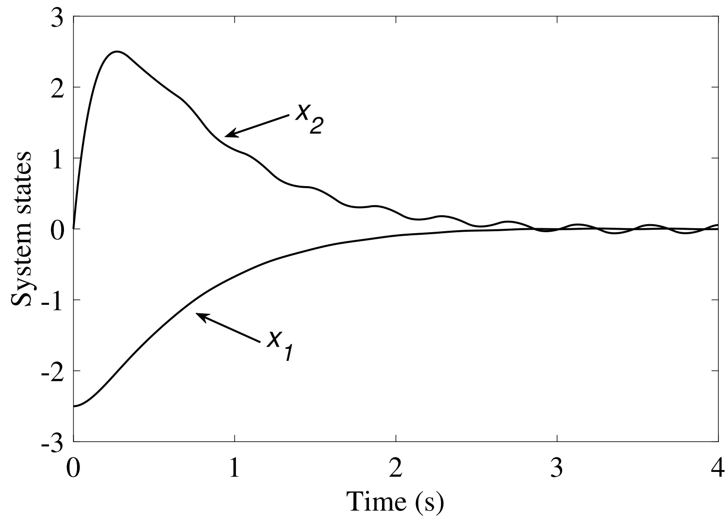

Figure 4.4: System states using the previous control approach.

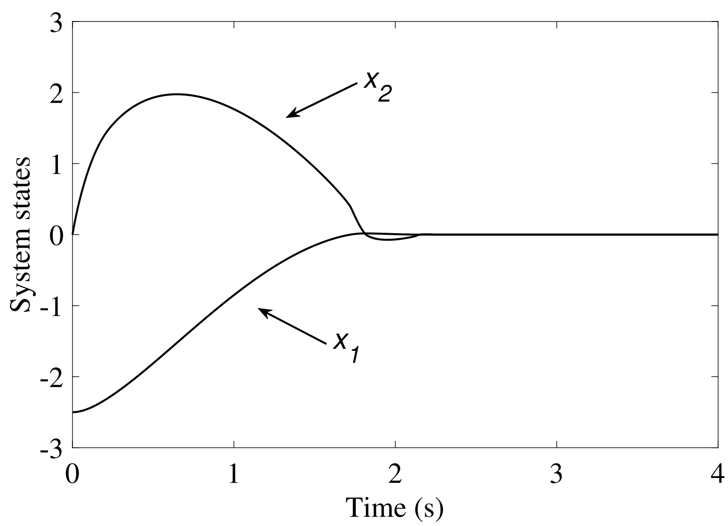

Figure 4.5: System states using the proposed control approach.

It can be deduced that by using the proposed control method, the system states could be convergence to zero, and the control signal is smooth without

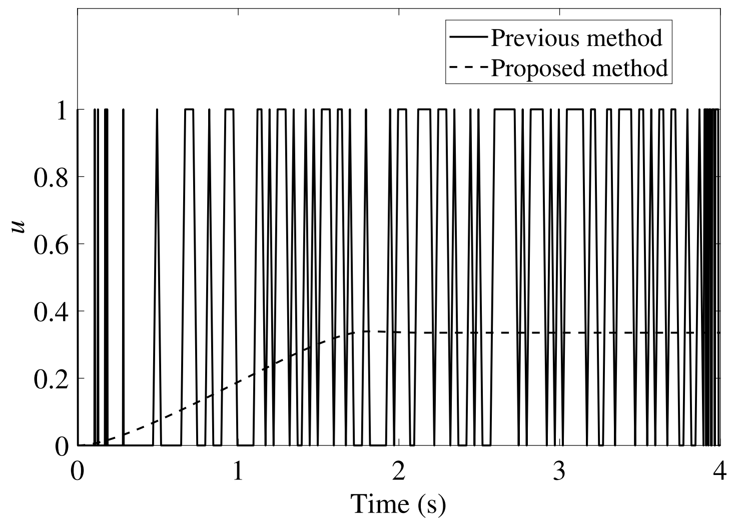

Figure 4.6: Control input of the previous method and proposed method.

chattering compared with previous method. So the tracking performance is improved.

Tracking of output voltage

To consider the uncertainties of the WPT systems, input voltage to the buck circuit and the voltage on load in the WPT system are shown in Fig. 4.7 when M_{23} is changed from 7.5 μH to 6.5 μH. Besides, the output voltage and input voltage to the buck circuit in the WPT system are shown in Fig. 4.8 when M_{23} is changed from 7.5 μH to 10.5 μH.

It can be concluded that even though the uncertainties exist in the WPT system, the tracking performance can still be maintained when the proposed control design scheme is adopted.

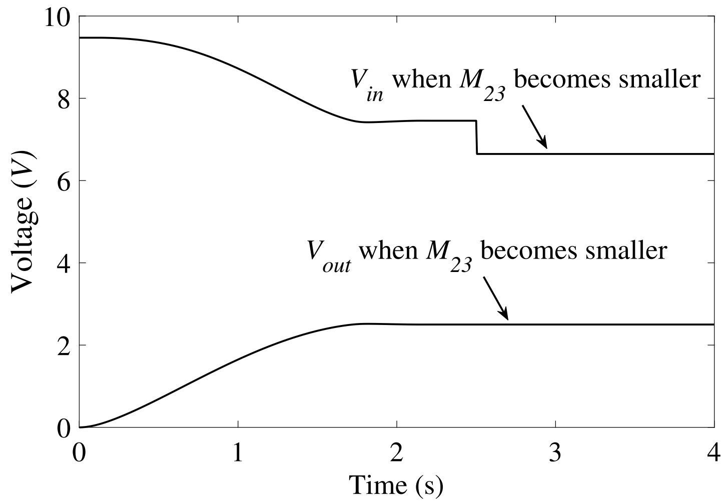

Figure 4.7: V_{out} and V_{in} when M_{23} becomes smaller.

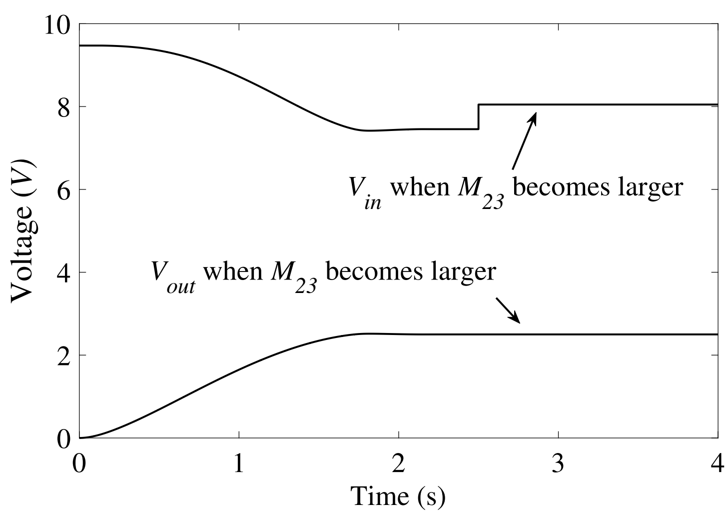

Figure 4.8: V_{out} and V_{in} when M_{23} becomes larger.

Robustness

To analyses the robust stability, the Lipschitz norm $\left\| [A(N + \Delta N) - AN] M^{-1} \right\|_{Lip}$ is depicted in Fig. 4.9.

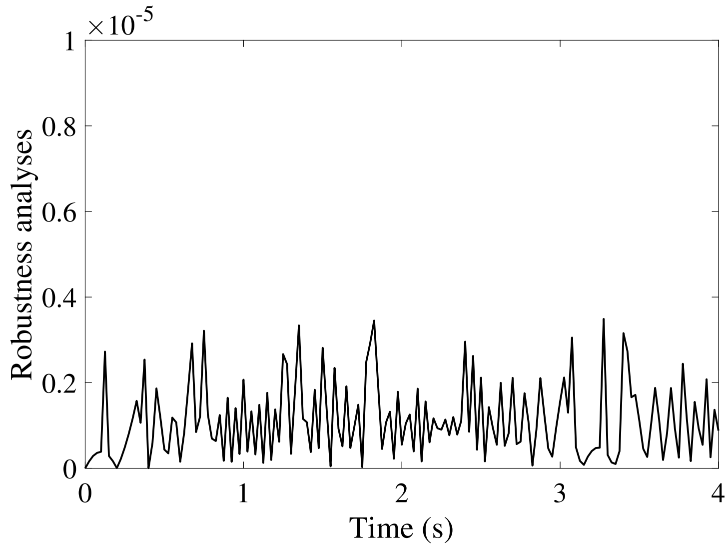

Figure 4.9: Robustness analyses.

It could be observed that the maximum value is less than 1, so the robustness is guaranteed by using the proposed operator-based nonlinear robust control system.

Noted that, the input power is 495 mW, the output power is 83 mW, so the transfer efficiency is 16.8 % in this WPT system.

4.4.2 Experiments

The comparison of tracking performance for the proposed method and previous method is shown in Fig. 4.10.

It can be deduced that the proposed nonlinear robust control scheme can improve the tracking performance on chattering problem.

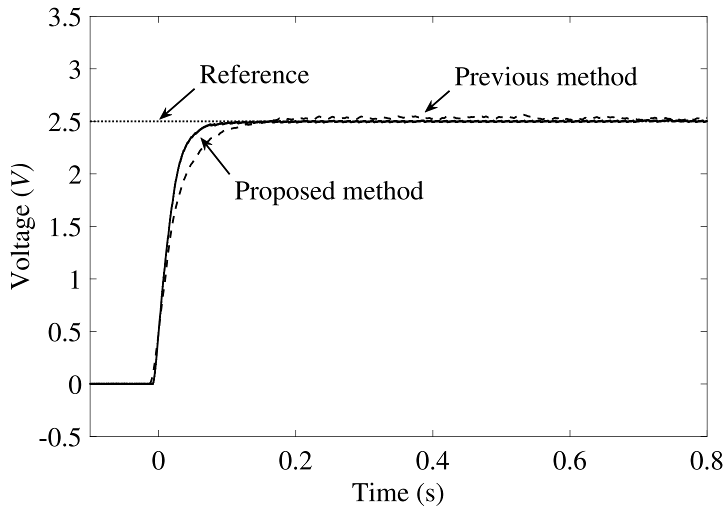

Figure 4.10: Tracking performance of previous method and the proposed method in setup.

To consider the uncertainties in the proposed control system, the output voltage and input voltage to buck circuit are depicted in Fig. 4.11 when the distance between transmit coil and receive coil changes from 50 mm to 54 mm. Besides, the output voltage and input voltage to buck circuit are depicted in Fig. 4.12 when the distance changes from 50 mm to 47 mm.

It can be obtained that even though the uncertainties exist in the WPT system, the tracking performance could still be maintained by using the proposed control design scheme.

Therefore, it could be observed from the results of simulations and experiments that the tracking performance is improved by using the proposed operator-based nonlinear robust control design scheme. Besides, the robust stability is guaranteed.

Noted that, the input power is 864 mW, the output power is 83 mW, so the transfer efficiency is 9.6 % in this WPT system due to the power loss on the DC-DC circuit (369 mW).

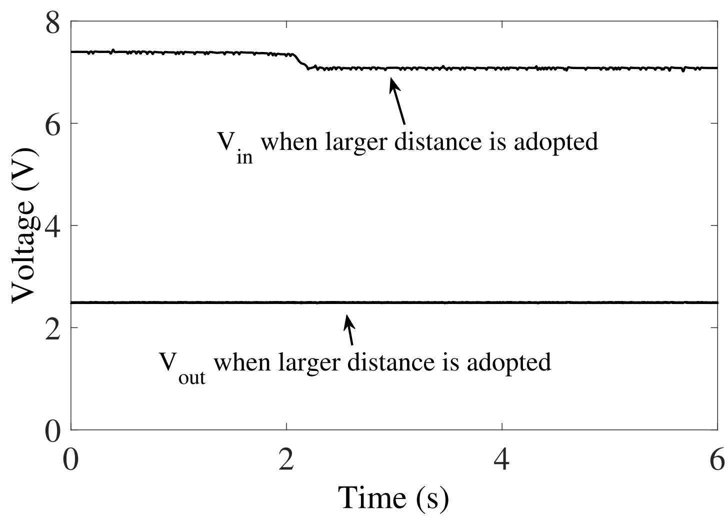

Figure 4.11: V_{out} and V_{in} when the distance becomes larger.

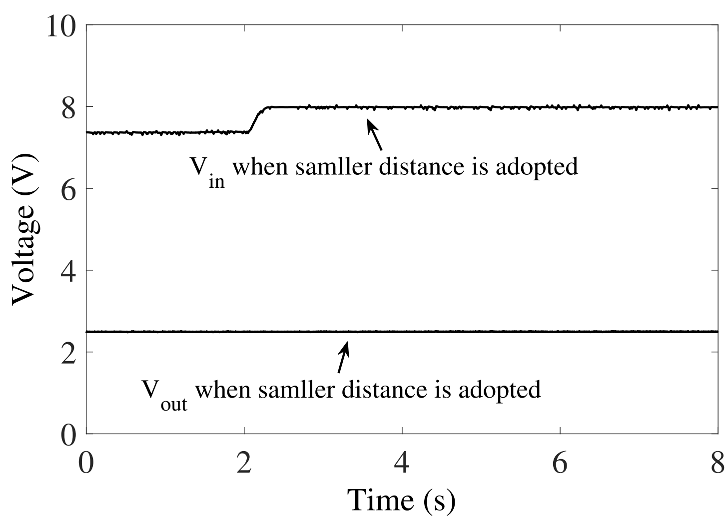

Figure 4.12: V_{out} and V_{in} when the distance becomes smaller.

4.5 Conclusion

In this chapter, a proposed new robust control design scheme for WPT systems with uncertainties was proposed based on operator theory. By using this proposed control design scheme, the robust stability can be guaranteed by using operator-based robust right coprime factorization approach. Moreover, the tracking performance is improved. Simulations and experiments were tested to confirm that this proposed control design system is effectiveness.

Chapter 5

Operator-based optimal equivalent load tracking control scheme for uncertain WPT systems

5.1 Introduction

In this chapter, the mathematical modeling of the WPT system including a boost circuit, an inverter circuit, the coupling system, a rectifier circuit and a buck circuit, is derived. And an optimal equivalent load tracking scheme for uncertain WPT systems is proposed based on operator theory. When the proposed control design scheme is adopted, the uncertain term could be dealt with by using the robust right coprime factorization approach, so the robust stability could be obtained. Then the optimal equivalent load for the coupling system can be matched to realize impedance matching without the acquisition of alternating current signal, thus the high efficiency could be obtained. Moreover, the reference signal of output voltage can be tracked.

In Section 5.2, first, the modeling of the mutual inductance and experimental verification are presented. Then the mathematical modeling of the

WPT systems including a boost circuit, an inverter circuit, the coupling system, a rectifier circuit and a buck circuit, is derived.

In Section 5.3, an optimal equivalent load tracking control scheme based on operator theory is proposed for WPT systems considering the uncertain term. By using the robust nonlinear control scheme, the robust stability of the feedback nonlinear control system is guaranteed by using robust right coprime factorization approach. Besides, the impedance matching could be obtained for the coupling system, so high efficiency can be achieved. Finally, the desired output voltage can be obtained.

In Section 5.4, simulations are conducted to confirm the effectiveness of the optimal equivalent load tracking control scheme based on operator theory.

In Section 5.5, the conclusion is presented.

5.2 Mathematical modeling of the WPT system with a boost circuit in the transmit side

5.2.1 Modeling of mutual inductance and experimental verification

In our setup, the radius of both the transmit coil and receive coil are 44mm, the turns of their coils are 20, and the axial lengths of the their coils are 10mm.

To obtain the mathematical modeling, a estimation method of the mutual inductance using the parameters of the setup need to be given. When the position of two coils are shown in Fig. 5.1, its equivalent circuit is as shown in Fig. 5.2, the mutual inductance could be calculated as follows.

$$M = \frac{2\mu_0 N_1 N_2}{\gamma}\sqrt{ab}\left[(1-\frac{\gamma^2}{2})F(\gamma) - E(\gamma)\right] \tag{5.1}$$

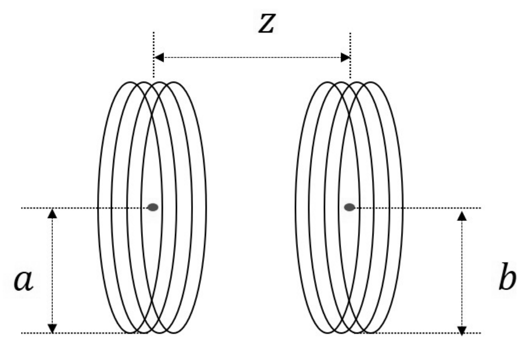

Figure 5.1: Position of the coupling coils.

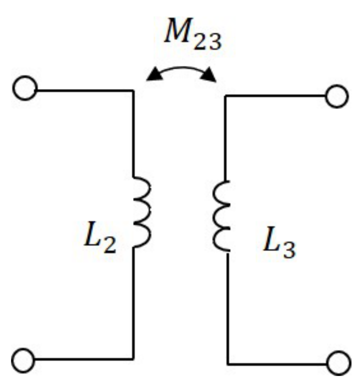

Figure 5.2: Modeling of the coupling coils.

where a and b are the radius of the two coils, c is the axial length of the coils, $d = (4a^2 + z^2)^{1/2}$, N_1 and N_2 are the number of turns of the two coils, μ_0 is the permeability of air, $\gamma^2 = \frac{4ab}{[(a+b)^2+z^2]}$, z is the distance between coils, and $F(\gamma)$ and $E(\gamma)$ are the elliptic integrals of the first and second kinds.

To obtain the values of $F(\gamma)$ and $E(\gamma)$, the method is as follows. Let

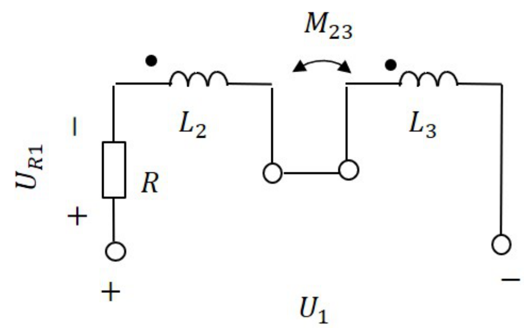

Figure 5.3: Coupling coils are connected in forward series.

$a_0 = 1$, $b_0 = (1 - \gamma^2)^{0.5}$ and $c_0 = \gamma$. Then apply the recursion formulas

$$\begin{aligned} a_n &= 0.5(a_{n-1} + b_{n-1}) \\ b_n &= (a_{n-1} b_{n-1})^{1/2} \\ c_n &= 0.5(a_{n-1} - b_{n-1}) \end{aligned} \tag{5.2}$$

The formulas are iterated until $a_n = b_n$. $F(\gamma)$ and $E(\gamma)$ are obtained as

$$\begin{aligned} F(\gamma) &= \frac{\pi}{2a_n} \\ E(\gamma) &= F(\gamma)\left[1 - 0.5 \sum 2^n c_n^2\right] \end{aligned} \tag{5.3}$$

To analyse the effectiveness of calculation method, the experimental measurement is used as the reference. The method of the experimental measurement is as follows. Firstly, when the coils are connected as Fig. 5.3, the equivalent inductor in this circuit is $L_{c1} = L_2 + L_3 + 2 * M_{23}$. The voltage U_1 and U_{R1} can be measured, so L_{c1} can be calculated as follows.

$$L_{c1} = \frac{U_1 - U_{R1}}{d(U_{R1}/R)/dt} \tag{5.4}$$

Besides, when the coils are connected as Fig. 5.4, the equivalent inductor in the circuit is $L_{c2} = L_2 + L_3 - 2 * M_{23}$. By using the same way, the L_{c2} can

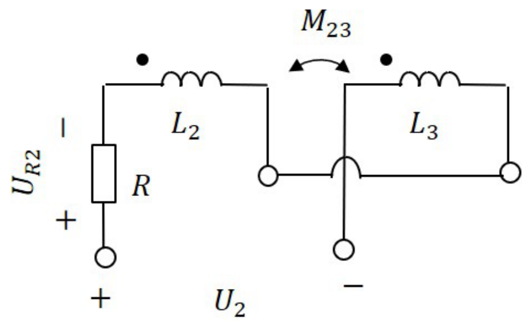

Figure 5.4: Coupling coils are connected in reverse series.

be calculated as follows.

$$L_{c2} = \frac{U_2 - U_{R2}}{d(U_{R2}/R)/dt} \tag{5.5}$$

Then, by using (5.4) and (5.5), the mutual inductor can be calculated as $M_{23} = \dfrac{L_{c1} - L_{c2}}{4}$.

The comparisons of the two methods are as shown in Fig. 5.5. It can be observed that the derivations are less than 10 %. Therefore, the calculation method of the the mutual inductance with respect to the distance between the resonant coils are verified to be effectiveness.

5.2.2 Modeling of WPT system

The WPT system used in this chapter consists of a boost circuit, an inverter circuit, the coupling system, a rectifier circuit and a buck circuit. The WPT system is shown in Fig. 5.6.

For simplicity, the modeling of the WPT as shown in Fig. 5.6 is derived under the three assumptions: 1. The buck and boost circuit is considered to be lossless, 2. C_5 is big enough to stabilize V_{inb}, 3. Only the first harmonic

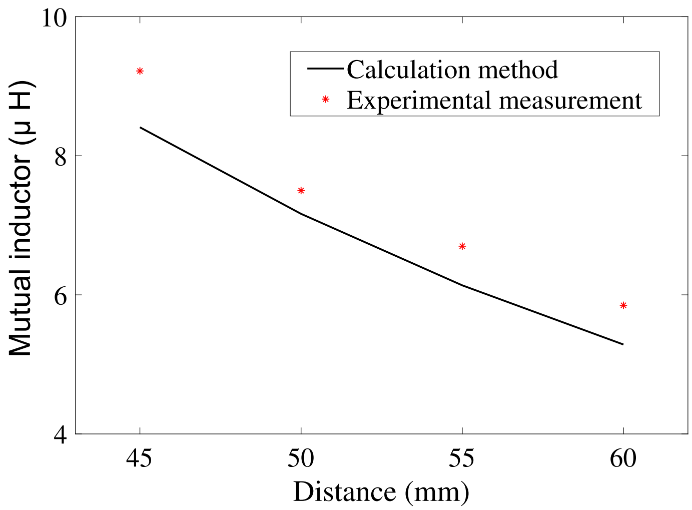

Figure 5.5: Mutual inductance by using the calculation method and experiment measurement.

of square waveform is taken into consideration, 4. The transit state of the boost circuit is not considered.

Define D_3 and D_4 be the duty cycles of switch S_1 and S_2. When the boost circuit of the wireless power system is considered, the following equations could be obtained in steady state.

$$V_{inv} = \frac{1}{1 - D_4} V_{in} \tag{5.6}$$

To consider the influence of the inverter shown in Fig. 5.7. The inverter is operated as follows, S_3, S_6 are controlled by plus signal g_1 which frequency is 2MHz and duty cycle is 50%, S_4, S_5 are controlled by signal by plus signal g_2 which delay half period of g_1. So the inverter could generate a square waveform satisfying that $\|V_{inc}\| = V_{inv}$ and $f = 2\ MHz$.

It should be noted that only ac signal could be used in the coupling system. Due to assumption 3, define V_s be the first harmonic waveform of V_{inc} and V_1 is the amplitude of V_s, so the following equation could be obtained

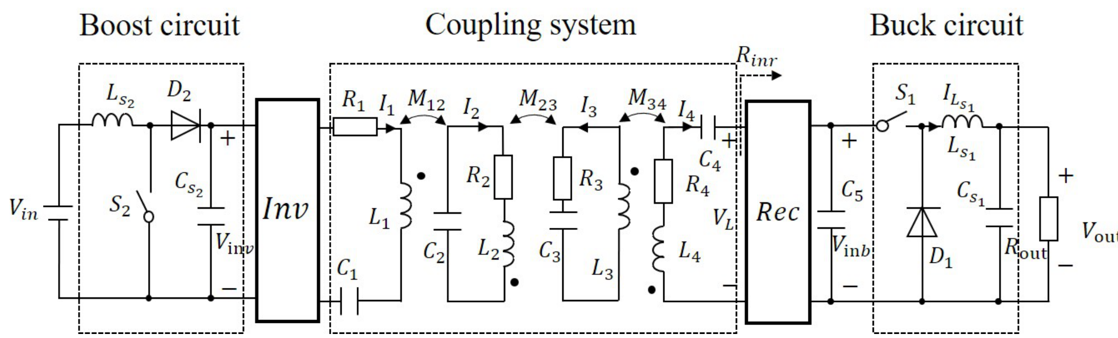

Figure 5.6: Diagram of the WPT system.

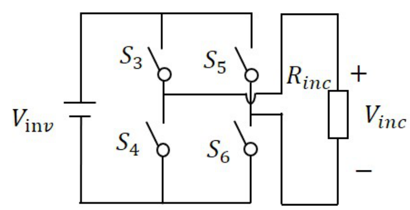

Figure 5.7: Circuit diagram of the inverter.

by using (5.6).

$$V_1 = \frac{4}{\pi} V_{inv} = \frac{4}{\pi(1 - D_4)} V_{in} \tag{5.7}$$

Then by using Kirchhoff's voltage law, define R_{inr} be the equivalent AC load of the rectifying circuit and buck circuit, the mathematical modeling of the coupling system can be obtained as follows.

$$I_1 \left(R_1 + jwL_1 + \frac{1}{jwC_1} \right) + jwI_2M_{12} = V_s \tag{5.8}$$

$$I_2 \left(R_2 + jwL_2 + \frac{1}{jwC_2} \right) + jw \left(I_1M_{12} - I_3M_{23} \right) = 0 \tag{5.9}$$

$$I_3 \left(R_3 + jwL_3 + \frac{1}{jwC_3} \right) + jw \left(I_4M_{34} - I_2M_{23} \right) = 0 \tag{5.10}$$

$$I_4 \left(R_{inr} + R_4 + jwL_4 + \frac{1}{jwC_4} \right) + jwI_3M_{34} = 0 \tag{5.11}$$

where $w = 2\pi f$.

Define that V_{ac} is the first harmonic waveform of the V_L and V_2 is the amplitude of V_{ac}, $V_{ac} = I_4 R_{inr}$ can be solved using the above four KVL equations, where $wL_i = \dfrac{1}{wC_i}(i = 1, 2, 3, 4)$

$$\begin{aligned}
V_{ac} &= \frac{jw^3 M_{12} M_{23} M_{34} R_{inr} V_s}{w^4 M_{12}^2 M_{34}^2 + Z_1 Z_2 Z_3 Z_4 + w^2 \kappa} \\
Z_1 &= R_1 + jwL_1 + \frac{1}{jwC_1} \\
Z_2 &= R_2 + jwL_2 + \frac{1}{jwC_2} \\
Z_3 &= R_3 + jwL_3 + \frac{1}{jwC_3} \\
Z_4 &= R_{inr} + R_4 + jwL_4 + \frac{1}{jwC_4} \\
\kappa &= M_{12}^2 Z_3 Z_4 + M_{23}^2 Z_1 Z_4 + M_{34}^2 Z_1 Z_2
\end{aligned} \tag{5.12}$$

Due to the stabilize function of C_5, the top value V_{L1} and the low value V_{L2} of V_L (which is a square waveform) can be obtained using a Fourier method.

$$V_{L1} = -V_{L2} = \frac{\pi}{4} V_2 \tag{5.13}$$

Then V_{in} can be obtained as follows using (5.7) and (5.12).

$$V_{inb} = \frac{w^3 M_{12} M_{23} M_{34} R_{inr} V_{in}}{(1 - D_4)\left(w^4 M_{12}^2 M_{34}^2 + Z_1 Z_2 Z_3 Z_4 + w^2 \kappa\right)} \tag{5.14}$$

It should be noted that V_{inb} contains the equivalent AC resistance R_{inr} which is unknown.

Then the assignment is to obtain R_{inr}. Under the above assumptions, the input of the rectifying circuit consists of an ideal sinusoidal current driven from the resonant and a square wave voltage as for the large capacitor. The relationship between I_4 and I_{out}, the relationship between V_{ac} and V_{out} can be obtained as follows.

$$I_4 = \frac{\pi}{2} D_3 I_{out} sin\ \theta \tag{5.15}$$

$$V_{ac} = \frac{4V_{out}}{\pi D_3} sin\ \theta. \tag{5.16}$$

Therefore, R_{inr} can be calculated as follows.

$$R_{inr} = V_{ac}/I_4 = \frac{8R_{out}}{(\pi D_3)^2} \tag{5.17}$$

Besides, to consider the transient response of the buck circuit, the modeling of the WPT system is as follows.

$$\frac{dI_{L_{s_1}}}{dt} = \frac{1}{L_{s_1}} \left(u_1 V_{inb} - V_{out}\right) \tag{5.18}$$

$$\frac{dV_{out}}{dt} = \frac{1}{C_{s_1}} \left(I_{L_{s_1}} - \frac{V_{out}}{R_{out}}\right) \tag{5.19}$$

By define the following functions.

$$\begin{aligned}
M_1 &= -\frac{1}{2R_{out}C_{s_1}} \\
N_1 &= \sqrt{\frac{1}{(2R_{out}C_{s_1})^2} - \frac{1}{C_{s_1}L_{s_1}}} \\
X_1 &= M_1 + N_1 \\
Y_1 &= M_1 - N_1 \\
M_2 &= D_3 V_{inb} \frac{M_1 - N_1}{2N_1} \\
N_2 &= -D_3 V_{inb} \frac{M_1 + N_1}{2N_1}
\end{aligned} \tag{5.20}$$

Then the modeling of such WPT systems could be obtained as follows by solving (5.19).

$$V_{out} = M_2 e^{X_1 t} + N_2 e^{Y_1 t} + u_1 V_{inb} \tag{5.21}$$

Where V_{inb} is expressed as (5.14), M_2, N_2, X_1 and Y_1 are defined in (5.20), u_1 and D_4 are the duty cycles of S_1 and S_2.

It should be noted that, by calculating the derivation of the coupling system's efficiency with respect to R_{inr}, where the optimal load R_{ref} of R_{inr} to maximize the efficiency (realize impedance matching) should satisfy the following equation.

$$\frac{(wM_{34})^2}{R_{ref}+R_4} = R_3\sqrt{1+\frac{(wM_{23})^2}{R_2R_3}} \tag{5.22}$$

So the optimal load R_{ref} could be calculated using (5.22) as follows.

$$R_{ref} = \frac{\sqrt{R_2R_3}\cdot(wM_{34})^2}{R_3\cdot\sqrt{R_2R_3+(wM_{23})^2}} \tag{5.23}$$

5.3 Proposed operator-based optimal equivalent load tracking scheme

In this subsection, the proposed optimal equivalent load tracking scheme based on operator theory for uncertain wireless power transfer systems is depicted in Fig. 5.8. In this control design scheme, A and B^{-1} are the designed operators to guarantee the robust stability of the control system by using robust right coprime factorization approach. Besides, K_2, C_1 and χ_1 are designed to track the optimal equivalent load by controlling the duty cycle of the buck circuit. Moreover, by controlling the duty cycle of the boost circuit, C_2 and K_1 are the designed so that the desired output voltage could be obtained.

To consider the uncertain term ΔP of the WPT system, the mathematical modeling plant $P+\Delta P$ could be expressed as follows.

$$y = (1+\Delta)\left(M_2e^{X_1t}+N_2e^{Y_1t}+D_3V_{inb}\right) \tag{5.24}$$

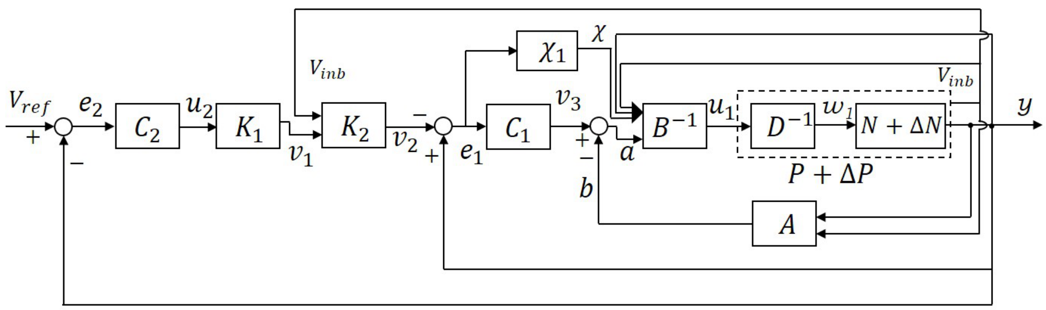

Figure 5.8: Proposed control design scheme.

where $\|\Delta\| < 1$, y is the output voltage V_{out}.

The plant could be factorized as follows.

$$N + \Delta N: \quad y = (1+\Delta)\Big((1-w_1)\, V_{inb} \frac{M_1 - N_1}{2N_1} e^{X_1 t} - (1-w_1)\Big) V_{inb} \frac{M_1 + N_1}{2N_1} e^{Y_1 t} + (1-w_1)\, V_{inb} \tag{5.25}$$

$$D: \quad u_1 = 1 - w_1 \tag{5.26}$$

To guarantee the robust stability of nonlinear system, the operators A and B are designed as follows.

$$A: \quad b = 1 - \Big[\frac{C_{s_1} L_{s_1}}{V_{inb}} \big(\frac{d^2 y}{dt^2} + \frac{y}{C_{s_1} L_{s_1}} + \frac{1}{R_{out} C_{s_1}} \frac{dy}{dt}\big)\Big] \tag{5.27}$$

$$B^{-1}: \quad u = \frac{\mathbf{sgn}(v) + 1}{2} \tag{5.28}$$

where K is a designed desired satisfying $K > 1$, **sgn** means the sign of the signal, u is the transit state of switch S_1 ($u = 0$ means S_1 is off and $u = 1$ means S_1 is on), noted that u_1 is the equivalent control of u in the switch-mode control system, and

$$v = a + 1 - D_3 - \chi \tag{5.29}$$

The proposed controllers C_1 and χ_1 are designed as follows.

$$C_1: \quad v_3 = e_1 + K \tag{5.30}$$

$$\chi_1: \quad \chi = \alpha e_1 + \dot{e}_1 + K \tag{5.31}$$

where α is a designed constant which is larger than 1.

So $w_1 = 1 - u_1 < 1$ could be obtained by using (5.26), $a = v - 1 + D_3 - \chi$ could be derived using (5.29), and A is designed as the inverse function of N ($A = N^{-1}$). Besides, $e_1 = \dot{e}_1 = 0$ and $v = 0$ could be obtained by using the proposed control design system, it will be discussed later. Then the operator $\tilde{M}$ could be calculated by using the deigned operators as follows.

$$\begin{aligned}
\tilde{M} &= (A(N + \Delta N) + BD)(w_1) \\
&= A(N + \Delta N)(w_1) + a \\
&= w_1 + \Delta \cdot w_1 + v - 1 + D_3 - \chi \\
&= w_1 + \Delta \cdot w_1 + v - 1 + D_3 + \alpha e + \dot{e} + K \\
&= K + \Delta \cdot w_1
\end{aligned} \tag{5.32}$$

So $\tilde{M}$ is an unimodular operator because of $K > 1$, $\|\Delta\| < 1$, and $w_1 < 1$. Besides, $M = K$ can be obtained without the uncertain term Δ.

Furthermore, to confirm the robust stability of the feedback nonlinear system, the Lipschitz norm in $\|[A\,(N + \Delta N) - AN]M^{-1}\|_{Lip}$ is

$$\begin{aligned}
&\|[A\,(N + \Delta N) - AN]M^{-1}\|_{Lip} \\
\leq &\|A\,(N + \Delta N) - AN\|_{Lip} \cdot \|M^{-1}\| \\
= &\|\Delta\| \cdot w_{eq} \cdot \frac{1}{K} \\
< &1.
\end{aligned} \tag{5.33}$$

Because both (2.16) and (2.17) are satisfied for the nonlinear control system, the robust stability is guaranteed by using operator-based robust right coprime factorization approach.

5.3.1 Proposed impedance matching control system

To realize the optimal equivalent load tracking control (impedance matching) for the uncertain WPT systems ($R_{inr} = R_{ref}$), firstly, the desired value of v_2 which could realize the optimal equivalent load tracking control is calculated with the uncertainties. Secondly, the tracking of the desired value is proved in mathematical way.

When the buck circuit is considered to be lossless and the output load does not vary, R_{ref} could be calculated using (5.23), the optimal duty cycle D_{3o} should satisfying the following equation to realize impedance matching.

$$D_{3o} = \sqrt{\frac{8R_{out}}{\pi^2 R_{ref}}} \tag{5.34}$$

However, the impedance matching could be destroyed when output load R_{out} varies.

To deal with the uncertain term in the WPT systems, the input voltage to the inverter circuit V_{inv}, the rectifier circuit V_{inb} and output voltage V_{out} in the control system are sampled in every transient state. The feedforward compensator χ_1, the sampled voltages V_{inb} and V_{out} work together to realize the tracking of v_2 as follows.

First, then the following equation could be obtained using (5.12).

$$V_2 = \frac{w^3 M_{12} M_{23} M_{34} R_{inr} V_1}{w^4 M_{12}^2 M_{34}^2 + Z_1 Z_2 Z_3 Z_4 + w^2 \kappa} \tag{5.35}$$

where V_1 is the amplitude of the sinusoidal voltage for the coupling system, V_2 is the amplitude of sinusoidal voltage for rectifier circuit satisfying that $V_2 = 4/\pi V_{inb}$.

Then the actual R_{inr} could be calculated as follows using V_{inb}, which could be acquired in simulation.

$$\begin{aligned} R_{inr} =& \frac{w^4 M_{12}^2 M_{34}^2 + R_1 R_2 R_3 R_4 + w^2 M_{12}^2 R_3 R_4}{X_3} \cdot V_2 \\ &+ \frac{w^2 M_{23}^2 R_1 R_4 + w^2 M_{34}^2 R_1 R_2}{X_3} \cdot V_2 \end{aligned} \tag{5.36}$$

where $X_3 = V_1 w^3 M_{12} M_{23} M_{34} - V_2 R_1 R_2 R_3 - V_2 w^2 M_{12}^2 R_3 - V_2 w^2 M_{23}^2 R_1$, $V_1 = 4V_{inv}/\pi$, and $V_2 = 4/\pi V_{inb}$.

So the proposed compensated controller K_2 to maintain impedance matching is designed as follows using (5.23), (5.34) and (5.36).

$$v_2 = V_{inb} D_{3o} \sqrt{\frac{R_{inr}}{R_{ref}}} \tag{5.37}$$

Where D_{3o} is the optimal duty cycle to realize impedance matching without considering the lossy of the buck circuit and the variation of output load. By using this proposed compensated controller K_2, the voltage v_2 could be considered as a constant value in steady state so that the impedance matching is realized considering the uncertain term of the WPT system.

The next assignment is to maker sure that v_2 could be tracked. As shown in Fig. 5.8, $a = v_3 - b$. Then v could be calculated as follows using (5.26) and (5.29).

$$\begin{aligned} v &= a + 1 - u_1 - \chi \\ &= (v_3 - b) + 1 - u_1 - (\alpha e_1 + \dot{e}_1 + K) \\ &= e_1 + K - w_1 + 1 - u_1 - (\alpha e_1 + \dot{e}_1) - K \\ &= -(\alpha - 1) e_1 - \dot{e}_1 \end{aligned} \tag{5.38}$$

The time derivative of v is

$$\dot{v} = -(\alpha - 1)\dot{e}_1 - \ddot{e}_1. \tag{5.39}$$

The modeling of N could be expressed as follows using (5.18), (5.19) and (5.26).

$$\ddot{e}_1 = -\frac{\dot{e}_1}{R_{out}C_{s_1}} + \frac{1}{L_{s_1}C_{s_1}}\Big[\big(1-w_1\big)V_{inb} - v_2 - e_1\Big] \tag{5.40}$$

Because the buck circuit always satisfying that $0 < V_{out} = v_2 + e_1 < V_{inb}$, the following equations could be obtained.

$$\dot{v} = -\frac{1}{L_{s_1}C_{s_1}}\left(V_{inb} - v_2 - e_1\right) < 0 \quad v > 0 \tag{5.41}$$

$$\dot{v} = \frac{1}{L_{s_1}C_{s_1}}\left(v_2 + e_1\right) > 0 \qquad\qquad v < 0 \tag{5.42}$$

So v could converge to zero when time comes to infinite, then w_1 could be obtained.

$$w_1 = 1 - \frac{v_2}{V_{inb}}. \tag{5.43}$$

Furthermore, due to both X_1 and Y_1 are negative numbers, the output voltage y could be obtained as follows when time comes to infinite.

$$\begin{aligned} y =& N(w_1) \\ =& \left(1-w_1\right)V_{inb}\frac{M_1 - N_1}{2N_1}e^{X_1 t} - \left(1-w_1\right) \\ & \cdot V_{inb}\frac{M_1 + N_1}{2N_1}e^{Y_1 t} + \left(1-w_1\right)V_{inb} \\ \rightarrow & v_2 \end{aligned} \tag{5.44}$$

Therefore, when the proposed control scheme is adopted, the tracking of optimal equivalent load can be obtained with consideration of the uncertain term in the WPT system.

5.3.2 Proposed output voltage tracking control system

As discussed above, the impedance matching could be realized, but the output voltage will vary when output load varies and V_1 is fixed. By changing the duty cycle of the boost circuit, V_1 is changeable with respect to the uncertainties so that the desired output voltage could be obtained. The proposed controller C_2 is designed as follows.

$$u_3 = \begin{cases} 1 & when\ e_2 > +h \\ 0 & when\ e_2 < -h \end{cases} \tag{5.45}$$

where u_3 is the transit state of switch S_2 ($u_3 = 0$ means S_2 is off and $u_3 = 1$ means S_2 is on). Then the desired duty cycle D_4 could be obtained to track the reference signal.

When the WPT system operators in steady state, to provide the corresponding V_1 using D_4, the controller K_1 is designed as

$$V_1 = \frac{\pi}{4(1 - D_4)} V_{in}. \tag{5.46}$$

So the desired output voltage could be obtained in the WPT system, and the V_1 for impedance matching is obtained.

Therefore, the robust stability of the feedback nonlinear system is guaranteed by using robust right coprime factorization approach. Besides, the impedance matching for the coupling system can be realized without the acquisition of AC signal. Moreover, the desired output voltage could be tracked.

5.4 Simulations

To confirm the effectiveness of the proposed control design scheme, the proposed WPT system is conducted using simulations. The simulations are conducted by using Matlab/Simulink (Simscape Electrical Toolbox), which could provide the electrical components to consider the dynamic of the WPT system. The WPT system using the proposed control method is as shown in Fig. 5.9. The parameters of the WPT system are given in Table. 5.1

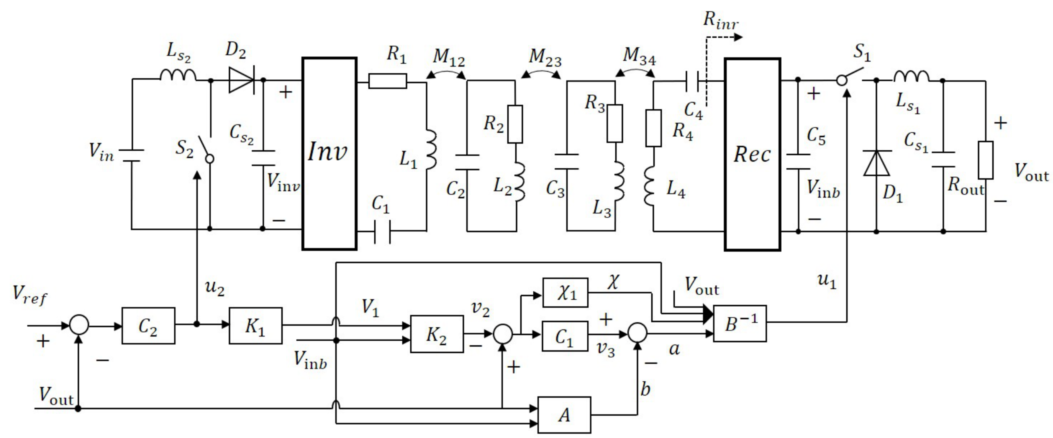

Figure 5.9: Diagram of the proposed control design WPT system.

and the designed parameters the proposed control methods are $V_{ref} = 2.5V$, $K = 1.32$, $\alpha = 14$ and $h = 0.02$.

The comparisons of time-domain transient output voltage and equivalent load by using both proposed method and previous method is shown in Figs. 5.10 and 5.11. It could be observed that the output voltage could be tracked by using both the two methods. Moreover, compared with the previous method, the error between the actual equivalent load and the desired equivalent load could be largely alleviated by using the the proposed method.

When there exists the uncertain term of the output load, the output voltage could be obtained by using both proposed control design scheme and the previous method as shown in Fig. 5.12. It could be observed that the reference signal could be tracked by using both the control schemes.

The equivalent load for the coupling system is shown in Fig. 5.13 when the uncertain term exists. It could be observed that the impedance matching could be realized by using the proposed control design scheme, but the previous method could not guarantee the impedance matching.

Table 5.1: Specifications in the WPT system.

Description	**Parameter**	**Value**
Source voltage	V_{in}	$5\ V$
Inductance of coil	$L_1,\ L_4$	$4.3\ \mu H$
	$L_2,\ L_3$	$35.3\ \mu H$
Mutual coefficient	$M_{12},\ M_{34}$	$8.5\ \mu H$
	M_{23}	$7.5\ \mu H$
Resonant capacitors	$C_2,\ C_3$	$179\ pF$
	$C_1,\ C_4$	$1\ nF$
Parasitic resistance	R_1, R_4	$1\ \Omega$
	$R_2,\ R_3$	$45\ \Omega$
Stabilization capacitor	C_5	$1\ \mu F$
Filter capacitor	C_{s_1}	$1000\ \mu F$
	C_{s_2}	$3000\ \mu F$
Filter inductance	L_{s_1}	$1\ mH$
	L_{s_2}	$2\ mH$
Output load	R_{out}	$85\ \Omega$

Then the efficiency of the WPT system is presented by using two methods is shown in Fig. 5.14. Due to the realization of impedance matching, the efficiency of the WPT system by using proposed control design scheme would be high when compared with the previous method.

The robust stability could be analyzed by using (2.17) in Fig.5.15. It could be seen that the maximum value of the Lipschitz norm is less than 1, so the robust stability of the control system is guaranteed by using operator-based robust right coprime factorization approach.

Therefore, by using the proposed control design scheme, the robust stability of the control design scheme is guaranteed. Moreover, the desired output voltage and impedance matching could be obtained, thus high efficiency is achieved at the same time.

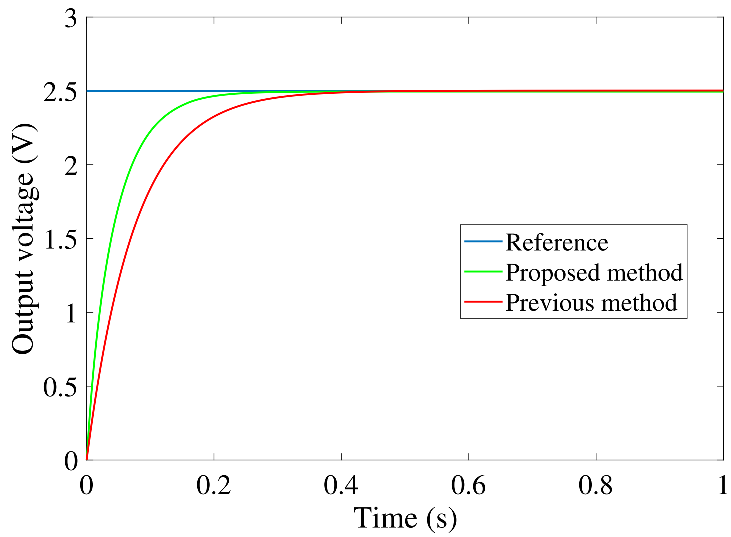

Figure 5.10: Comparison of transient output voltage by using proposed method and previous method.

5.5 Conclusion

In this chapter, the proposed optimal equivalent load tracking control scheme based on operator theory was presented for WPT systems with the uncertain term. The robust stability of the feedback nonlinear system was guaranteed by using robust right coprime factorization approach. Besides, the impedance matching of the WPT system can be obtained without the acquisition of the AC signal, so high efficiency was obtained and complexity of the setup can be erased. Moreover, the desired output voltage was obtained in the WPT system. Simulation results were shown to confirm that the proposed control design scheme is effectiveness.

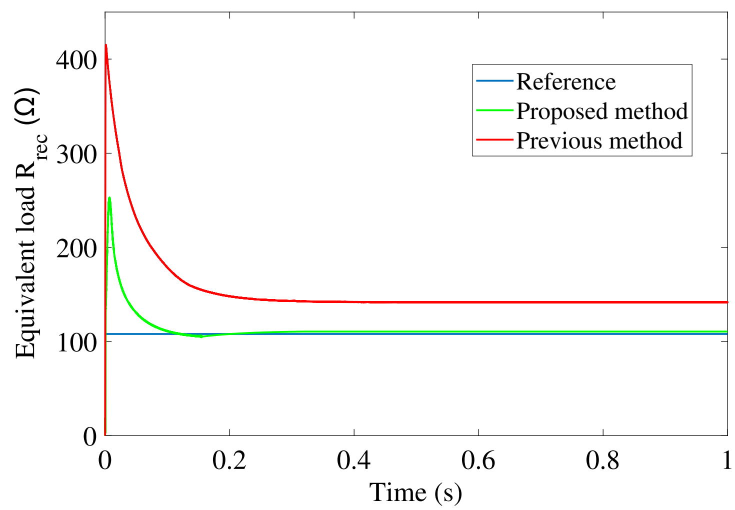

Figure 5.11: Comparison of transient equivalent load by using proposed method and previous method.

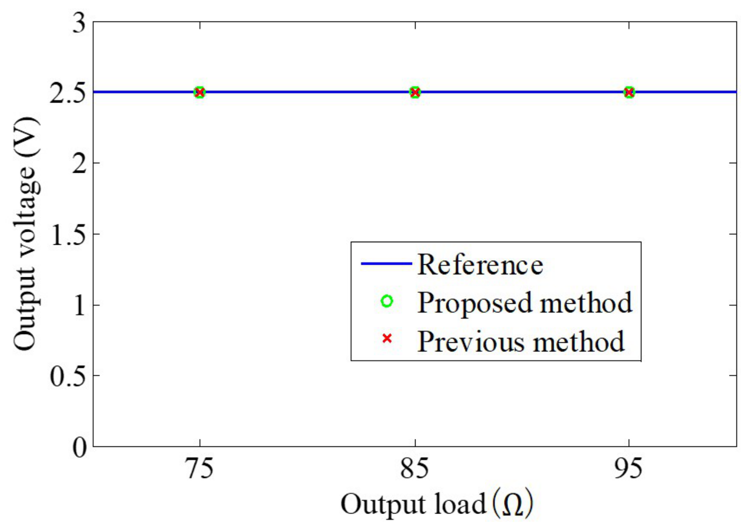

Figure 5.12: Output voltage with different output load.

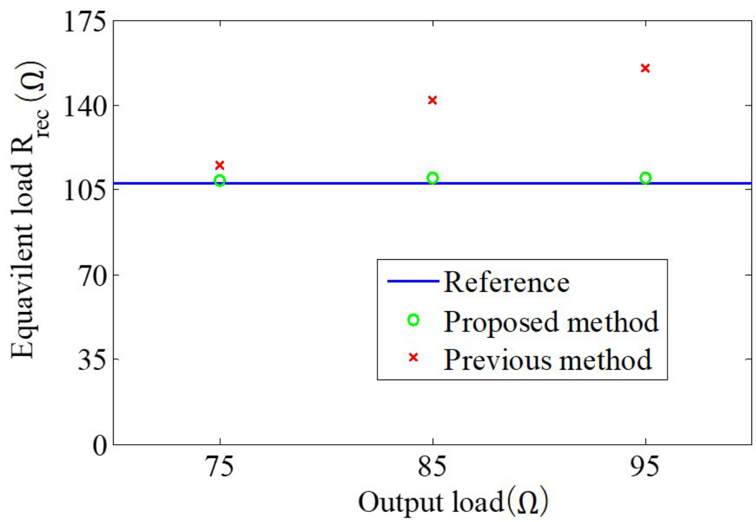

Figure 5.13: Equivalent load R_{rec} with different output load.

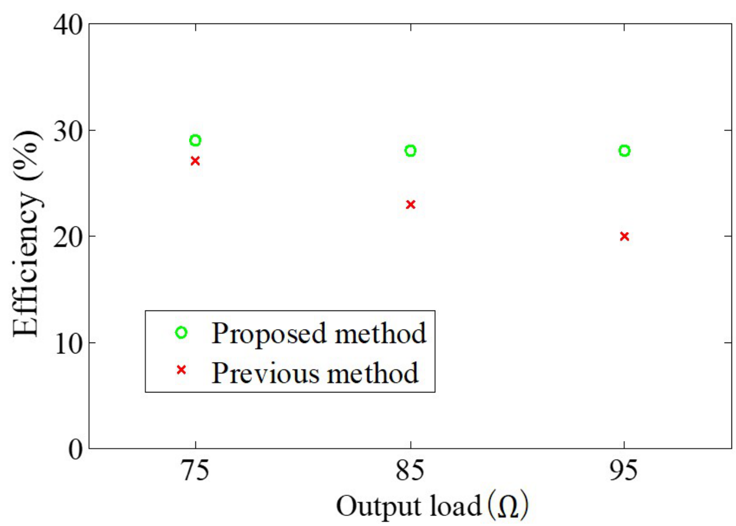

Figure 5.14: Efficiency of the WPT system with different output load.

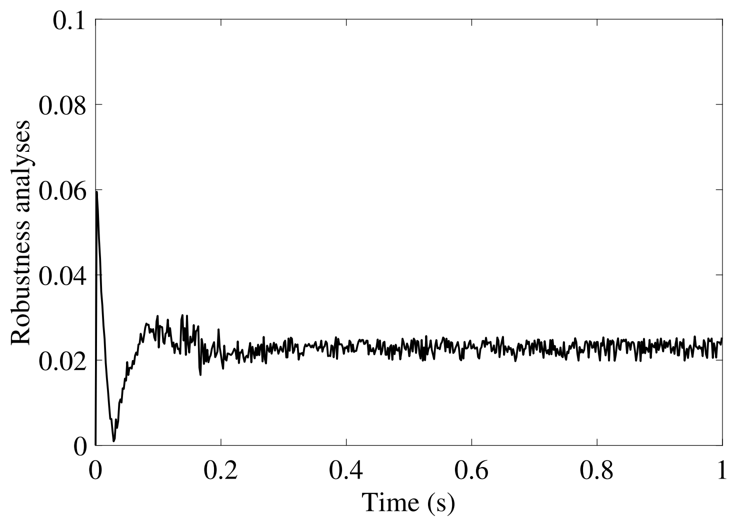

Figure 5.15: Robustness analyses.

Chapter 6

Conclusions

In this dissertation, the WPT systems driven by the duty cycle of switch were studied to propose methods, there are three problems need to tackled: the robust stability of the nonlinear system, the desired tracking performance and high efficiency at the same time. Three different robust nonlinear control methods were proposed in the dissertation.

In Chapter 2, the mathematical preliminaries about operator theory and the key theories in WPT systems were presented, circuit theory was introduced to analyse the power exchange between two resonance objects of the WPT systems, then the mathematical modeling of the buck circuit was given in its transient state. After that, basic definitions of operator-based right factorization, right coprime factorization, and robust right coprime factorization for nonlinear systems were given to analyse the robust stability of uncertain WPT systems. Moreover, the impedance matching theory using buck circuit was presented to obtain the high efficiency for WPT systems. Finally, the problems discussed in this dissertation were stated.

In Chapter 3, fist, the derivation about the mathematical modeling of WPT systems was given. Then motivated by the usefulness of operator theory for uncertain nonlinear systems, and rare previous research on WPT system were conducted considering the uncertain term resulting from the uncertain distance between coils. Besides, SMC method is a promising way to realize the tracking performance, it has the advantageous, such as fast-dynamic response and simple implement in setup. A robust nonlinear control design scheme based on operator theory was proposed to tackle the uncertain mutual inductor, which is resulting from the movement of transmit coil or receive coil. There are two advantages in the proposed control design system. First, in order to tackle the uncertain term, operator-based right coprime factorization approach was adopted to guarantee the robust stability of the nonlinear system. Then sliding mode technology was used to obtain the tracking performance of the nonlinear system. Finally, simulations and experiments are conducted to verify the effectiveness of the proposed control design scheme.

In Chapter 4, the chattering problem exists because of the inherent shortage about traditional SMC method in the designed control system mentioned in Section 3. Motivated by the elimination method of chattering phenomenon existing in traditional SMC method, the tracking performance could be improved. Then a proposed new robust control design scheme based on operator theory for WPT systems with uncertainties was proposed. In the proposed control design system, to deal with the uncertainties in the wireless power transfer system, operator-based robust right coprime factorization approach is adopted to guarantee the robust stability. Moreover, the tracking performance is improved by using the proposed control design scheme. Finally, results of simulations and experiments are presented to confirm the effectiveness of the proposed control design scheme.

In Chapter 5, the proposed control schemes in Sections 3 and 4 could guarantee tracking performance of output voltage for the robust WPT control system, but the impedance matching may be destroyed when the output load is varied, thus high efficiency could not be achieved. Besides, high frequency AC (alternating current) signal increase the complexity of the setup. Motivated by the power management of both transfer power and efficiency, not only the desired output voltage should be obtained, but also the impedance matching need to be realized considering the existence of uncertain term about the output load, and the acquisition of high frequency AC signal should be eliminated. So an optimal equivalent load tracking scheme based on operator theory for uncertain WPT systems was proposed. By using the proposed control scheme, the uncertain term could be dealt with by using the robust right coprime factorization approach, so the robust stability can be obtained. After that, the optimal equivalent load for the coupling system can be tuned to realize impedance matching without the acquisition of AC current signal, thus the high efficiency was obtained. Moreover, the reference signal of output voltage can be tracked. Simulation results show the effectiveness of this proposed control method.

In conclusion, three operator-based robust nonlinear control design schemes for WPT systems were proposed in this dissertation. The first control scheme was to ensure the tracking performance and robust stability at the same time for the uncertain nonlinear WPT systems, it focus on ensuring the robust stability of the uncertain WPT systems using robust right coprime factorization. After that, the second control scheme was proposed to improve the tracking performance of the uncertain WPT systems, it focus on eliminating the chattering problem of the uncertain WPT systems. Finally, not only the robust stability of the nonlinear control system was guaranteed by using the third control scheme, but also the desired output voltage and optimal equivalent load can be obtained, thus the desired output power and high efficiency using operator-based robust nonlinear control design scheme at the same time. Simulations and/or experiments results were presented to confirm the effectiveness of the three proposed control schemes.

In our future work, the experimental setup will be build, and the third proposed control design scheme will be tested in the setup to verify its effectiveness. Besides, the optimal parameters of the proposed operator-based robust nonlinear WPT systems will be considered based on ant colony optimization and other optimization method [96–98].

Bibliography

[1] H. Rakouth, J. Absmeier, A. Brown, et al. EV charging through wireless power transfer: Analysis of efficiency optimization and technology trends. *Proceedings of the FISITA 2012 World Automotive Congress*, pp. 871-884, Berlin, Heidelberg, 2013.

[2] N. Tesla, *Apparatus for transmitting electrical energy*, U.S. Patent 1 119 732, 1914.

[3] J. T. Howell, M. J. O'Neill, and R. L. Fork, Advanced receiver/converter experiments for laser wireless power transmission. *In Solar Power from Space-SPS'04*, vol. 567, no. 99, pp. 187-194, 2004.

[4] N. Shinohara, Power without wires, *IEEE Microwave Magazine*, vol. 12, no. 7, pp. S64-S73, 2011.

[5] W. C. Brown, Status of the microwave power transmission components for the solar power satellite, *IEEE Transactions on Microwave Theory and Techniques*, vol. 29, no.12, pp. 1319-1327, 1981.

[6] A. Sample, and J. R. Smith, Experimental results with two wireless power transfer systems, *In Proceedings of IEEE Radio and Wireless Symposium*, pp. 16-18, San Diego, USA, 2009.

[7] J. O. McSpadden, and J. C. Mankins, Space solar power programs and microwave wireless power transmission technology, *IEEE Microwave Magazine*, vol. 3, no. 4, pp. 46-57, 2002.

[8] J. L. Villa, J. Sallan, J. F. Sanz, and A. Llombart, High-misalignment tolerant compensation topology for ICPT systems, *IEEE Transactions on Industrial Electronics*, vol. 59, no. 2, pp. 945-951, 2012.

[9] J. Sallan, J. L. Villa, A. Llombart, and J. F. Sanz, Optimal design of ICPT systems applied to electric vehicle battery charge, *IEEE Transactions on Industrial Electronics*, vol. 56, no. 6, pp. 2140-2149, 2009.

[10] J. L. Villa, J. Sallan, A. Llombart, and J. F. Sanz, Design of a high frequency inductively coupled power transfer system for electric vehicle battery charge, *Applied Energy*, vol. 86, no. 3, pp. 355-363, 2009.

[11] C. S. Wang, O. H. Stielau, and G. A. Covic, Design considerations for a contactless electric vehicle battery charger, *IEEE Transactions on Industrial Electronics*, vol. 52, no. 5, pp. 1308-1314, 2005.

[12] C. S. Wang, G. A. Covic, and O. H. Stielau, Power transfer capability and bifurcation phenomena of loosely coupled inductive power transfer systems, *IEEE Transactions on Industrial Electronics*, vol. 51, no. 1, pp. 148-157, 2004.

[13] O. H. Stielau, and G. A. Covic, Design of loosely coupled inductive power transfer systems, *Proceedings of International Conference on Power System Technology*, pp. 85-90, Perth, Australia, 2000.

[14] Z. Pantic and S. M. Lukic, Framework and topology for active tuning of parallel compensated receivers in power transfer systems, *IEEE Transactions on Power Electronics*, vol. 27, no. 11, pp. 4503-4513, 2012.

[15] A. Kurs, A. Karalis, R. Moffatt, J.D. Joannopoulos, P. Fisher, and M. Soljacic, Wireless power transfer via strongly coupled magnetic resonances, *Science*, vol. 317, no. 5834, pp. 83-86, 2007

[16] W. Q. Niu, W. Gu, J. X. Chu, and A. D. Shen, Coupled-mode analysis of frequency splitting phenomena in CPT systems, *Electronics Letters*, vol. 48, no. 12, pp. 723-724, 2012.

[17] C. J. Chen, T. H. Chu, C. L. Lin, and Z. C. Jou, A study of loosely coupled coils for wireless power transfer, *IEEE Transactions on Circuits and Systems II: Express Briefs*, vol. 57, no. 7, pp. 536-540, 2010.

[18] M. Kiani, U. M. Jow, and M. Ghovanloo, Design and optimization of a 3-coil inductive link for efficient wireless power transmission, *IEEE Transactions on Biomedical Circuits and Systems*, vol. 5, pp. 579-591, 2011.

[19] R. J. Sedwick, Long range inductive power transfer with superconducting oscillators, *Annals of Physics*, vol. 325, no. 2, pp. 287-299, 2010.

[20] Yin, N., Xu, G., Yang, et al, Analysis of wireless energy transmission for implantable device based on coupled magnetic resonance, *IEEE Transactions on Magnetics*, vol. 48, no. 2, pp. 723-726, 2012.

[21] M. Kiani, and M Ghovanloo, The circuit theory behind coupled-mode magnetic resonance-based wireless power transmission, *IEEE Trans. Circuits Syst. I: Regul. Pap.*, vol. 59, no. 9, pp. 2065-2074, 2012.

[22] Y. Zhai, Y. Sun, X. Dai, Y. Su, and Z. Wang, Modeling and analysis of magnetic resonance wireless power transmission systems, *Chinese Society for Electrical Engineering*, vol. 32, no. 12, pp. 155-160, 2012.

[23] A. Kurs, R. Moffatt, and M. Soljacic, Simultaneous mid-range power transfer to multiple devices, *Applied Physics Letters*, vol. 96, no. 4, 044102, 2010.

[24] F. Zhang, S. A. Hackworth, W. Fu, C. Li, Z. Mao, and M. Sun, Relay effect of wireless power transfer using strongly coupled magnetic resonances, *IEEE Transactions on Magnetics*, vol. 47, no. 5, pp. 1478-1481, 2011.

[25] J. J. Casanova, Z. N. Low, and J. Lin, A loosely coupled planar wireless power system for multiple receivers, *IEEE Transactions on Industrial Electronics*, vol. 56, no. 8, pp. 3060-3068, 2009.

[26] K. Lee and D. H. Cho, Diversity analysis of multiple transmitters in wireless power transfer system, *IEEE Transactions on Magnetics*, vol. 49, no. 6, pp. 2946-2952, 2013.

[27] Q. Xu, H. Wang, Z. Gao, Z. H. Mao, J. He, and M. Sun, A novel mat-based system for position-varying wireless power transfer to biomedical implants, *IEEE Transactions on Magnetics*, vol. 49, no. 8, pp. 4774-4779, 2013.

[28] L. Xie, Y. Shi, Y. T. Hou, and H. D. Sherali, Making sensor networks immortal: An energy-renewal approach with wireless power transfer, *IEEE/ACM Transactions on networking*, vol. 20, no. 6, pp. 1748-1761, 2012.

[29] T. Imura, H. Okabe, and Y. Hori, Basic experimental study on helical antennas of wireless power transfer for electric vehicles by using magnetic resonant couplings, *Proceedings of IEEE Vehicle Power and Propulsion Conference*, pp. 936-940, Dearborn, USA, 2009.

[30] Y. D. Ko and Y. J. Jang, The optimal system design of the online electric vehicle utilizing wireless power transmission technology, *IEEE Transactions on Intelligent Transportation Systems*, vol. 14, no. 3, pp. 1255-1265, 2013.

[31] T. C. Beh, M. Kato, T. Imura, S. Oh, and Y. Hori, Automated impedance matching system for robust wireless power transfer via magnetic resonance coupling, *IEEE Transactions on Industrial Electronics*, vol. 60, no. 9, pp. 3689-3698, 2013.

[32] J. Park, Y. Tak, Y. Kim, Y. Kim, and S. Nam, Investigation of adaptive matching methods for near-field wireless power transfer, *IEEE Transactions on Antennas and Propagation*, vol. 59, no. 5, pp. 1769-1773, 2011.

[33] L. Tan, X. Huang, H. Huang, Y. Zou, and H. Li, Transfer efficiency optimal control of magnetic resonance coupled system of wireless power transfer based on frequency control, *Science China Technological Sciences*, vol. 54, no. 6, pp. 1428-1434, 2011

[34] A. Sample, B. H. Waters, S. T. Wisdom, and J. R. Smith, Enabling seamless wireless power delivery in dynamic environments, *Proceedings of the IEEE*, vol. 101, no. 6, pp. 1343-1358, 2013.

[35] W. S. Lee, W. I. Son, K. S. Oh, and J. W. Yu, Contactless energy transfer systems using antiparallel resonant loops, *IEEE Transactions on Industrial Electronics*, vol. 60, no. 1, pp. 350-359, 2013.

[36] W. Fu, B. Zhang, and D. Qiu, Study on frequency-tracking wireless power transfer system by resonant coupling, *Proceedings of IEEE 6th International Conference on Power Electronics and Motion Control*, pp. 2658-2663, Wuhan, China, 2009.

[37] T. P. Duong and J. W. Lee, Experimental results of high-efficiency resonant coupling wireless power transfer using a variable coupling method, *IEEE Microwave and Wireless Components Letters*, vol. 21, no. 8, pp. 442-444, 2011.

[38] A. Sample, D. Meyer, and J. Smith, Analysis, experimental results, and range adaptation of magnetically coupled resonators for wireless power transfer, *IEEE Transactions on Industrial Electronics*, vol. 58, no. 2, pp. 544-554, 2011.

[39] D. Ahn and S. Hong, A study on magnetic field repeater in wireless power transfer, *IEEE Transactions on Industrial Electronics*, vol. 60, no. 1, pp. 360-371, 2013.

[40] X. Zhang, Q. Yang, H. Chen, Y. Li, X. Zhang, and L. Jin, Research on characteristics of frequency splitting in electromagnetic coupling resonant power transmission systems. *Chinese Society for Electrical Engineering*, vol. 32, no. 9, pp. 167-172, 2012.

[41] Y. Li, Q. Yang, Z. Yan, H. Y. Chen, X. Zhang, L. Jin, and M. Xue, Characteristic of frequency in wireless power transfer system via magnetic resonance coupling, *Electric Machines and Control*, vol. 16, no. 7, pp. 7-11, 2012.

[42] T. Diekhans and R. Doncker, A dual-side controlled inductive power transfer system optimized for large coupling factor variations and partial load, *IEEE Transactions on Power Electronics*, vol. 30, no. 11, pp. 6320-6328, 2015.

[43] A. Ali, M. H. Saied, M. Z. Mostafa, and T. M. Abdel-Moneim, A survey of maximum PPT techniques of PV systems, *Proceedings of IEEE Energytech*, pp. 1-17, Cleveland, USA, 2012.

[44] T. Paing, J. Shin, R. Zane, and Z. Popovic, Resistor emulation approach to low-power RF energy harvesting, *IEEE Transactions on Power Electronics*, vol. 23, no. 3, pp. 1494-1501, 2008.

[45] D. Ahn, S. Kim, J. Moon, and I. K. Cho, Wireless power transfer with automatic feedback control of load resistance transformation, *IEEE Transactions on Power Electronics*, vol. 31, no. 11, pp. 7876-7886, 2016.

[46] N. A. Keeling, G. A. Covic, and J. T.Boys, A unity-power-factor IPT pickup for high-power applications, *IEEE Transactions on Industrial Electronics*, vol. 57, no. 2, pp. 744-751, 2010.

[47] W. Zhong and S. Hui, Maximum energy efficiency tracking for wireless power transfer systems, *IEEE Transactions on Power Electronics*, vol. 30, no. 7, pp. 4025-4034, 2015.

[48] Y. Yang, W. Zhong, S. C. Tan, and S. Hui, Dynamic improvement of wireless power transfer systems with maximum energy efficiency tracking by sliding mode control, *Proceedings of IEEE Future Energy Electronics Conference and ECCE*, pp. 1736-1740, Kaohsiung, Taiwan, 2017.

[49] B. L. Cannon, J. F. Hoburg, D. D. Stancil, and S. C. Goldstein, Magnetic resonant coupling as a potential means for wireless power transfer to multiple small receivers, *IEEE Transactions on Power Electronics*, vol. 24, no. 7, pp. 1819-1825, 2009.

[50] S. Bi, M. Deng, and Y. Xiao, Robust stability and tracking for operator-based nonlinear uncertain systems, *IEEE Transactions on Automation Science and Engineering*, vol. 12, no. 3, pp. 1059-1066, 2015.

[51] G. Chen, and Z. Han, Robust right coprime factorization and robust stabilization of nonlinear feedback control systems, *IEEE Transactions on Automatic Control*, vol. 43, no. 10, pp. 1505-1509, 1998.

[52] M. Deng, *Operator-based nonlinear control systems design and applications*, 1st ed., Wiley-IEEE Press, 2014.

[53] M. Deng, A. Inoue, and K. Ishikawa, Operator-based nonlinear feedback control design using robust right coprime factorization, *IEEE Transactions on Automatic Control*, vol. 51, no. 4, pp. 645-648, 2006.

[54] D. Zhang, P. Shi, and L. Yu, Containment control of linear multiagent systems with aperiodic sampling and measurement size reduction, *IEEE Transactions on Neural Networks and Learning Systems*, vol. 29, no. 10, pp. 1-10, 2018.

[55] D. Zhang, L. Lu, and F. Gang, Consensus of heterogeneous linear multi-agent systems subject to aperiodic sampled-data and DoS attack, *IEEE Transactions on Cybernetics*, DOI:10.1109/TCYB.2018.2806387, 2018.

[56] Y. Hu, S. Ge, and C. Su, Stabilization of uncertain nonholonomic systems via time-varying sliding mode control, *IEEE Transactions on Automatic Control*, vol. 49, no. 5, pp. 757-763, 2004.

[57] H. Komurcugil, Non-singular terminal sliding-mode control of DC-DC buck converters, *Control Engineering Practice*, vol. 21, no. 3, pp. 321-332, 2013.

[58] V. Utkin, J. Guldner, and J. Shi, *Sliding mode control in electro-mechanical systems*, CRC press, 2009.

[59] J. Yang, S. Li, and X. Yu, Sliding-mode control for systems with mismatched uncertainties via a disturbance observer, *IEEE Transactions on Industrial Electronics*, vol. 60, no. 1, pp. 160-169, 2013.

[60] X. Yu and O. Kaynak, Sliding mode control made smarter: A computational intelligence perspective, *IEEE Systems, Man, and Cybernetics Magazine*, vol. 3, pp.31-34, 2017.

[61] Z. Wang, Y. Li, Y. Sun, C. Tang, and X. Lv, Load detection model of voltage-fed inductive power transfer system. *IEEE Transactions on Power Electronics*, vol. 28, no. 11, pp. 5233-5243, 2013.

[62] H. Li, J. Li, K. Wang, W. Chen, and Y. Xu, A maximum efficiency point tracking control scheme for wireless power transfer systems using magnetic resonant coupling, *IEEE Transactions on Power Electronics*, vol. 30, no. 7, pp.3998-4008, 2015

[63] T. Hiramatsu, X. Huang, M. Kato, T. Imura, and Y. Hori, Independent control of maximum transmission efficiency by the transmitter side and power by the receiver side for wireless power transfer, *IEEJ Transactions on Industry Applications*, vol. 135, pp.847-854, 2015 (in Japanese)

[64] X. Gao, K. Masaki, M. Deng, and L. Jin, Nonlinear feedback control design based on operator theory for loosely coupled wireless power transfer systems, *Proceedings of IEEE International Conference on Advanced Mechatronic Systems*, pp. 230-235, 2016.

[65] X. Gao and M. Deng, Operator-based robust nonlinear control of an uncertain wireless power transfer system using sliding mode technology, *Transactions of the Institute of Measurement and Control*, vol.40, no. 6, pp. 43974406, 2018.

[66] X. Gao and M. Deng, Tracking performance improvement for operator-based nonlinear robust control of wireless power transfer systems with uncertainties, *International Journal of Control, Automation, and Systems*, vol. 17, pp. 1-10, 2019.

[67] X. Gao, M. Deng, and K. Masaki, Tracking operator-based optimal load control for loosely coupled wireless power transfer systems, *Proceedings of IEEE International Conference on Systems, Man, and Cybernetics*, pp. 2188-2193, Banff, Canada, 2017.

[68] X. Gao and M. Deng, Operator based robust nonlinear control of wireless power transfer systems against uncertainties, *Proceedings of the 2018 IEEJ Annual Conference on Electronics, Information and Systems*, pp. 1170-1175, September 5-8, 2018, Sapporo, Japan.

[69] X. Gao and M. Deng, An Operator-based Optimal Equivalent Load Tracking Control Scheme for Uncertain Wireless Power Transfer Systems, *IEEJ Transactions on Electronics, Information and Systems*, vol. 139, no. 4, 2019.

[70] A. Levant, Principles of 2-sliding mode design, *Automatica*, vol. 43, no. 4, pp. 576-586, 2007.

[71] K. S. Kim, Y. Park, and S. H. Oh, Designing robust sliding hyperplanes for parametric uncertain systems: a Riccati approach, *Automatica*, vol. 36, no. 7, pp. 1041-1048, 2000.

[72] H. H. Choi, An explicit formula of linear sliding surfaces for a class of uncertain dynamic systems with mismatched uncertainties, *Automatica*, vol. 34, no. 8, pp. 1015-1020, 1998.

[73] J. L. Chang, Dynamic output integral sliding-mode control with disturbance attenuation, *IEEE Transactions on Automatic Control*, vol. 54, no. 11, pp. 2653-2658, 2009.

[74] V. Utkin and J. Shi, Integral sliding mode in systems operating under uncertainty conditions, *Proceedings of IEEE Conference on Decision and Control*, pp. 4591-4596, Kobe, Japan, 1996.

[75] B. Beltran, T. Ahmed-Ali, and M. E. H. Benbouzid, High-order sliding-mode control of variable-speed wind turbines, *IEEE Transactions on Industrial Electronics*, vol. 56, no. 9, pp. 3314-3321, 2009.

[76] X. Zhang, H. Su, L. Xiao, and J. Chu, Robust sliding mode control based on integral sliding surfaces, *Proceedings of American Control Conference*, pp. 4074-4077, Oregon, USA, 2005.

[77] S. C. Tan, Y. M. Lai, M. K. Cheung, and C. K Tse, On the practical design of a sliding mode voltage controlled buck converter, *IEEE Transactions on Power Electronics*, vol. 20, no. 2, pp. 425-437, 2005.

[78] M. Deng, C. Jiang, A. Inoue, and C. Y. Su, Operator-based robust control for nonlinear systems with Prandtl-Ishlinskii hysteresis, *International Journal of Systems Science*, vol. 42, no. 4, pp. 643-652, 2011.

[79] M. Deng and T. Kawashima, Adaptive nonlinear sensorless control for an uncertain miniature pneumatic curling rubber actuator using passivity and robust right coprime factorization, *IEEE Transactions on Control Systems Technology*, vol. 24, no. 1, pp. 318-324, 2016.

[80] S. Wen and M. Deng, Operator-based robust nonlinear control and fault detection for a Peltier actuated thermal process, *Mathematical and Computer Modelling*, vol. 57, no. 2, pp. 16-29, 2013.

[81] Y. Wu and M. Deng, Operator-based robust nonlinear optimal vibration control for an L-shaped arm driven by linear pulse motor, *International Journal of Control, Automation and Systems*, vol. 15, no. 5, pp. 2026-2033, 2017.

[82] M. Deng and A. Wang, Robust non-linear control design to an ionic polymer metal composite with hysteresis using operator-based approach,

IET Control Theory and Applications, vol. 6, no. 17, pp. 2667-2675, 2012.

[83] N. Bu and M. Deng, System design for nonlinear plants using operator-based robust right coprime factorization and isomorphism, *IEEE Transactions on Automatic Control*, vol. 56, no. 4, pp. 952-957, 2011.

[84] M. Deng and N. Bu, Robust control for nonlinear systems using passivity-based robust right coprime factorization, *Proceedings of American Control Conference*, vol. 57, no. 10, pp. 2599-2604, 2012.

[85] F. Tao, M. Deng, and S. Bi, Practical design scheme for nonlinear systems with unknown bounded perturbations using robust right coprime factorization, *Proceedings of American Control Conference*, pp. 5942-5947, Chicago, USA, 2015.

[86] S. Bi, L. Wang, Y. Zhao, and M. Deng, Operator-based robust control for nonlinear uncertain systems with unknown backlash-like hysteresis, *International Journal of Control, Automation and Systems*, vol. 14, no. 2, pp. 469-477, 2016.

[87] Y. Wu and M. Deng, Experimental study on robust nonlinear forced vibration control for an L-shaped arm with reduced control inputs, *IEEE/ASME Transactions on Mechatronics*, vol. 22, no. 5, pp. 2186-2195, 2017.

[88] A. Wang, M. Deng, and D. Wang, Operator-based robust control design for a human arm-like manipulator with time-varying delay measurements, *International Journal of Control, Automation and Systems*, vol. 11, no. 6, pp. 1112-1121, 2013.

[89] A. Wang and M. Deng, Operator-based robust nonlinear tracking control for a human multi-joint arm-like manipulator with unknown time-

varying delays, *Applied Mathematics and Information Sciences*, vol. 6, no. 3, pp. 459-468, 2012.

[90] Y. Hong, G. Yang, D. Cheng, and S. Spurgeon, Finite time convergent control using terminal sliding mode, *Journal of Control Theory and Applications*, vol. 2, no. 1, pp. 69-74, 2004.

[91] S. P. Bhat and D. S. Bernstein, Geometric homogeneity with applications to finite-time stability, *Mathematics of Control, Signals and Systems*, vol. 17, no. 2, pp. 101-127, 2005.

[92] A. Isidori, *Nonlinear Control Systems*, 3rd edition, Springer Verlag, Berlin, 1995.

[93] Y. Feng, F. Han, and X. Yu, Chattering free full-order sliding-mode control, *Automatica*, vol. 50, no. 4, pp. 1310-1314, 2014.

[94] A. Babazadeh and D. Maksimovic, Hybrid digital adaptive control for fast transient response in synchronous buck DC-DC converters, *IEEE Transactions on Power Electronics*, vol. 24, no. 11, pp. 2625-2638, 2009.

[95] Y. Feng, X. Yu, and F. Han, On nonsingular terminal sliding-mode control of nonlinear systems, *Automatica*, vol. 49, no. 6, pp. 1715-1722, 2013.

[96] Q. Yang, W. Chen, Z. Yu, T. Gu, Y. Li, H. Zhang, and J. Zhang, Adaptive multimodal continuous ant colony optimization, *IEEE Transactions on Evolutionary Computation*, vol. 21, no. 2, pp. 191-205, 2017.

[97] Z. G. Chen, Z. H. Zhan, Y. Lin, Y. Gong, T. L. Gu, F. Zhao, H. Q. Yuan, X. Chen, Q. Li, and J. Zhang, Multiobjective cloud workflow scheduling: A multiple populations ant colony system approach, *IEEE Transactions on Cybernetics*, DIO: 10.1109/TCYB.2018.2832640, 2018.

[98] Y. J. Gong, E. Chen, Lionel M. Ni, et al, AntMapper: An ant colony-based map matching approach for trajectory-based applications, *IEEE Transactions on Intelligent Transportation Systems*, vol. 19, no. 2, pp. 390-401, 2018.

Publications

Journal papers

1. **X. Gao** and M. Deng, Operator-based Robust Nonlinear Control of an Uncertain Wireless Power Transfer System using Sliding Mode Technology, *Transactions of Institute of Measurement and Control*, vol. 40, no. 6, pp. 4397-4406, 2018. (Chapter 3)

2. **X. Gao** and M. Deng, Tracking Performance Improvement for Operator-Based Nonlinear Robust Control of Wireless Power Transfer Systems with Uncertainties, *International Journal of Control, Automation and Systems*, vol. 17, no. 3, pp. 545-554, 2019. (Chapter 4)

3. **X. Gao** and M. Deng, An Operator-based Optimal Equivalent Load Tracking Control Scheme for Uncertain Wireless Power Transfer Systems, *IEEJ Transactions on Electronics, Information and Systems*, vol. 139, no. 4, 2019. (Chapter 5)

Proceedings papers

1. **X. Gao**, M. Deng, K. Masaki, and L. Jin, Nonlinear feedback control design based on operator theory for loosely coupled wireless power transfer systems, *Proceedings of the 2016 International Conference on Advanced Mechatronic Systems*, pp. 230-235, November 30-December 3, 2016, Melbourne, Australia. (Chapter 3)

2. **X. Gao**, M. Deng, and K. Masaki, Tracking Operator-based Optimal Load Control for Loosely Coupled Wireless Power Transfer Systems, *Proceedings of the 2017 IEEE International Conference on Systems, Man, and Cybernetics*, pp. 2188-2193, October 5-8, 2017, Banff, Canada. (Chapter 5)

Other papers

1. **X. Gao**, M. Deng, and L. Jin, Operator based robust nonlinear control of wireless power transfer systems against uncertainties, *Proceedings of the 2018 IEEJ Annual Conference on Electronics, Information and Systems*, pp. 1170-1175, September 5-8, 2018, Sapporo, Japan.

2. K. Masaki, **X. Gao**, M. Deng, and Y. Noge, Operator-based integral sliding mode control design for WPT system via magnetic resonance coupling, *Proceedings of the 2017 International Conference on Advanced Mechatronic Systems*, pp. 429-434, December 6-9, 2017, Xiamen, China.

3. K. Masaki, **X. Gao**, M. Deng, and Y. Noge, Experimental study on operator-based integral sliding mode robust nonlinear control for WPT systems, *Proceedings of the 2018 IEEE International Conference on Intelligence and Safety for Robotics*, pp. 385-388, August 24-27, 2018, Shenyang, China.

4. K. Masaki, M. Deng, **X. Gao**, and Y. Noge, Operator based robust nonlinear control of wireless power transfer systems against uncertainties, *Proceedings of the 2017 IEEJ Annual Conference on Control*, pp. 41-44, August 26, 2017, Tokyo, Japan. (in Japanese)